Journal of Volcanology and Geothermal Research 259 (2013) 389–413

Contents lists available at SciVerse ScienceDirect

Journal of Volcanology and Geothermal Research

journal homepage: www.elsevier.com/locate/jvolgeores

Voluminous ice-rich and water-rich lahars generated during the 2009 eruption of Redoubt Volcano, Alaska

Christopher F. Waythomas [a,*], Thomas C. Pierson [b], Jon J. Major [b], William E. Scott [b]

[a] USGS, Alaska Volcano Observatory, 4210 University Drive, Anchorage AK 99508, USA
[b] USGS, Cascades Volcano Observatory, 1300 SE Cardinal Court, Building 10, Suite 100, Vancouver WA 98683-9589, USA

ARTICLE INFO

Article history:
Received 4 June 2011
Accepted 22 May 2012
Available online 31 May 2012

Keywords:
Redoubt Volcano
Lahars
Hazards
Volcano–ice interactions

ABSTRACT

Redoubt Volcano in south-central Alaska began erupting on March 15, 2009, and by April 4, 2009, had produced at least 20 explosive events that generated multiple plumes of ash and numerous lahars. The 3108-m-high, snow- and ice-clad stratovolcano has an ice-filled summit crater that is breached to the north. The volcano supports about 4 km^3 of ice and snow and about 1 km^3 of this makes up the Drift glacier on the north side of the volcano. Explosive eruptions between March 23 and April 4, which included the destruction of at least two lava domes, triggered significant lahars in the Drift River valley on March 23 and April 4, and several smaller lahars between March 24 and March 31. Mud-line high-water marks, character of deposits, areas of inundation, and estimates of flow velocity revealed that the lahars on March 23 and April 4 were the largest of the eruption. In the 2-km-wide upper Drift River valley, average flow depths were at least 2–5 m. Average peak-flow velocities were likely between 10 and 15 $m s^{-1}$, and peak discharges were on the order of 10^4–10^5 $m^3 s^{-1}$. The area inundated by lahars on March 23 was at least 100 km^2 and on April 4 about 125 km^2. Two substantial lahars emplaced on March 23 and one on April 4 had volumes on the order of 10^7–10^8 m^3 and were similar in size to the largest lahar of the 1989–90 eruption. The two principal March 23 lahars were primarily flowing slurries of snow and ice derived from Drift glacier and the Drift River valley where seasonal snow and tabular blocks of river ice were entrained and incorporated into the lahars. Despite morphologic evidence of two lahars, only a single deposit up to 5 m thick was found in most places and it contained about 80–95% of poorly sorted, massive to imbricate assemblages of snow and ice clasts. The deposit was frozen soon after it was emplaced and later eroded and buried by the April 4 lahar. The lahar of April 4, in contrast, was primarily a hyperconcentrated flow, as interpreted from 1- to 6-m-thick deposits of massive to horizontally stratified sand to fine gravel. Rock material in the April 4 lahar deposit is predominantly juvenile andesite, whereas rock material in the March 23 deposit is rare and not obviously juvenile. We infer that the lahars generated on March 23 were initiated by a rapid succession of vent-clearing explosions that blasted through about 50–100 m of crater-filling glacier ice and snow, producing a voluminous release of meltwater from Drift glacier. The resulting surge of water entrained snow, fragments of glacier and river ice, and river water along its flow path. Small-volume pyroclastic flows, possibly associated with destruction of a small dome or minor eruption-column collapses, may have contributed additional meltwater to the March 23 lahars. Meltwater generated by subglacial hydrothermal activity and stored beneath Drift glacier may have been ejected or released rapidly as well. The April 4 lahar was initiated when hot dome-collapse pyroclastic flows entrained and swiftly melted snow and ice on Drift glacier. The resulting meltwater incorporated pyroclastic debris and rock material from Drift glacier to form the largest lahar of the 2009 eruption. The peak discharge of the April 4 lahar was in the range of 60,000–160,000 $m^3 s^{-1}$. For comparison, the largest lahar of the 1989–90 eruption had a peak discharge of about 80,000 $m^3 s^{-1}$. Lahars generated by the 2009 eruption led to significant channel aggradation in the lower Drift River valley and caused extensive inundation at an oil storage and transfer facility located there. The April 4, 2009, lahar was 6–30 times larger than the largest meteorological floods known or estimated in the Drift River drainage.

© 2012 Published by Elsevier B.V.

1. Introduction

1.1. Setting

Redoubt Volcano is a historically active, andesite to dacite stratocone in the Cook Inlet region of Alaska (Fig. 1) that experienced

* Corresponding author.
E-mail address: chris@usgs.gov (C.F. Waythomas).

0377-0273/$ – see front matter © 2012 Published by Elsevier B.V.
doi:10.1016/j.jvolgeores.2012.05.012

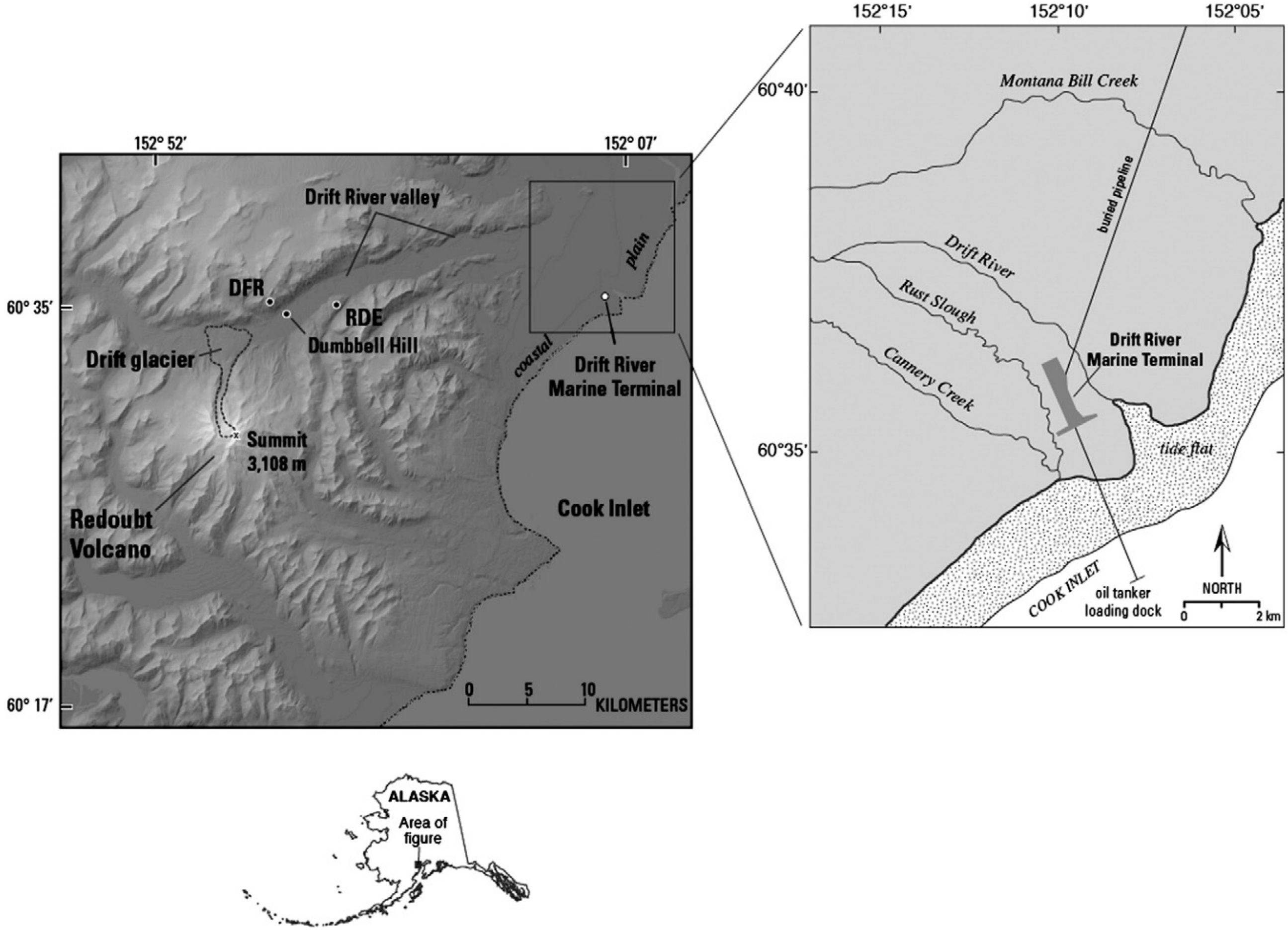

Fig. 1. Shaded relief map of Redoubt Volcano and the Drift River valley. The location of the Drift River Marine Terminal and seismic stations DFR and RDE also are shown. Inset map on right shows location of Montana Bill Creek, Rust Slough, Cannery Creek, and main channel of the lower Drift River.

its most recent eruption in March–July 2009 (Schaefer, 2012; Bull and Buurman, 2013). Prior to the start of the 2009 eruption, the volcano supported about 4 km^3 of glacier ice and perennial snow (Trabant and Hawkins, 1997), about 1 km^3 of which formed the Drift glacier on the north flank of the volcano (Figs. 1, 2). Downstream of the glacier, the Drift River flows 35 km eastward to Cook Inlet. The Drift River has a wide braided channel that occupies a 1.5- to 2.5-km-wide valley in its bedrock-confined upper and middle reaches. The lower 10 km of the valley is less confined and broadens over a narrow coastal plain where it is as much as 9 km wide and includes several distributary channels (Fig. 1).

Redoubt Volcano has erupted more than 50 times in the past 10,000 years and four times since 1900 (Beget and Nye, 1994; Till et al., 1994; Schiff et al., 2010). All of the known historical eruptive activity, and probably several prehistoric eruptions, have occurred from vents within the breached, 1 × 2 km, ice-filled summit crater at the head of the Drift glacier (Fig. 2). Each of the three eruptions since the 1960's (1966–68, 1989–90, 2009), produced multiple lahars in the Drift River valley (Sturm et al., 1986; Dorava and Meyer, 1994; Schaefer, 2012). Lahars associated with these recent eruptions have inundated significant parts of the lower Drift River and associated distributary channels. The lahars produced during the 1989–90 and 2009 eruptions have posed a significant hazard to oil-production infrastructure located near the mouth of the Drift River—both to pipelines buried beneath the river and to the Drift River Marine Terminal (DRMT), an oil storage and transfer facility (Fig. 1).

Redoubt Volcano began erupting in 2009 with a small phreatic explosion on March 15. A series of 19 discrete explosive events from late evening on March 22 (AKDT) through April 4 produced at least five pyroclastic flows and at least 20 lahars (Fig. 3) before the eruption transitioned to its final effusive phase that ended about July 1 (Schaefer, 2012; Bull and Buurman, 2013). Almost all lahars, recognized in seismic data, were triggered by rapid melting of ice and snow that typically occurred within minutes of explosions from the vent. The largest lahars occurred on March 23, March 26, and April 4. The lahars generated on March 23 contained significant amounts of river and glacier ice and were distinctly different in character compared to the watery lahars of March 26 and April 4. Two lahars produced on March 23 and one on April 4 overtopped and flowed around flood protection structures at the DRMT. Resulting deposits of mud, vegetation, and ice severely affected operations at the facility but did not cause any oil spills (Schaefer, 2012). In this paper we describe and characterize the largest flows, estimate their peak discharges and volumes, discuss their contrasting compositions and origins, and provide an updated context for future lahar hazards in the Drift River valley.

1.2. Lahars at snow- and ice-clad volcanoes

Mass flows composed of variable mixtures of sediment, ice, and water are expected consequences of eruptions at snow- and ice-clad volcanoes, including most of the historically active volcanoes in Alaska (Major and Newhall, 1989). Such flows, known as lahars, typically are classified as one of two types according to their proportions of solids and water: debris flows (about 50–75% solids by volume) and hyperconcentrated flows (about 10–50% solids by volume) (Vallance, 2000; Pierson, 2005). Mass flows having solid components that are dominated by ice fragments (including ice-rich lahars, ice-slurry flows, snow-

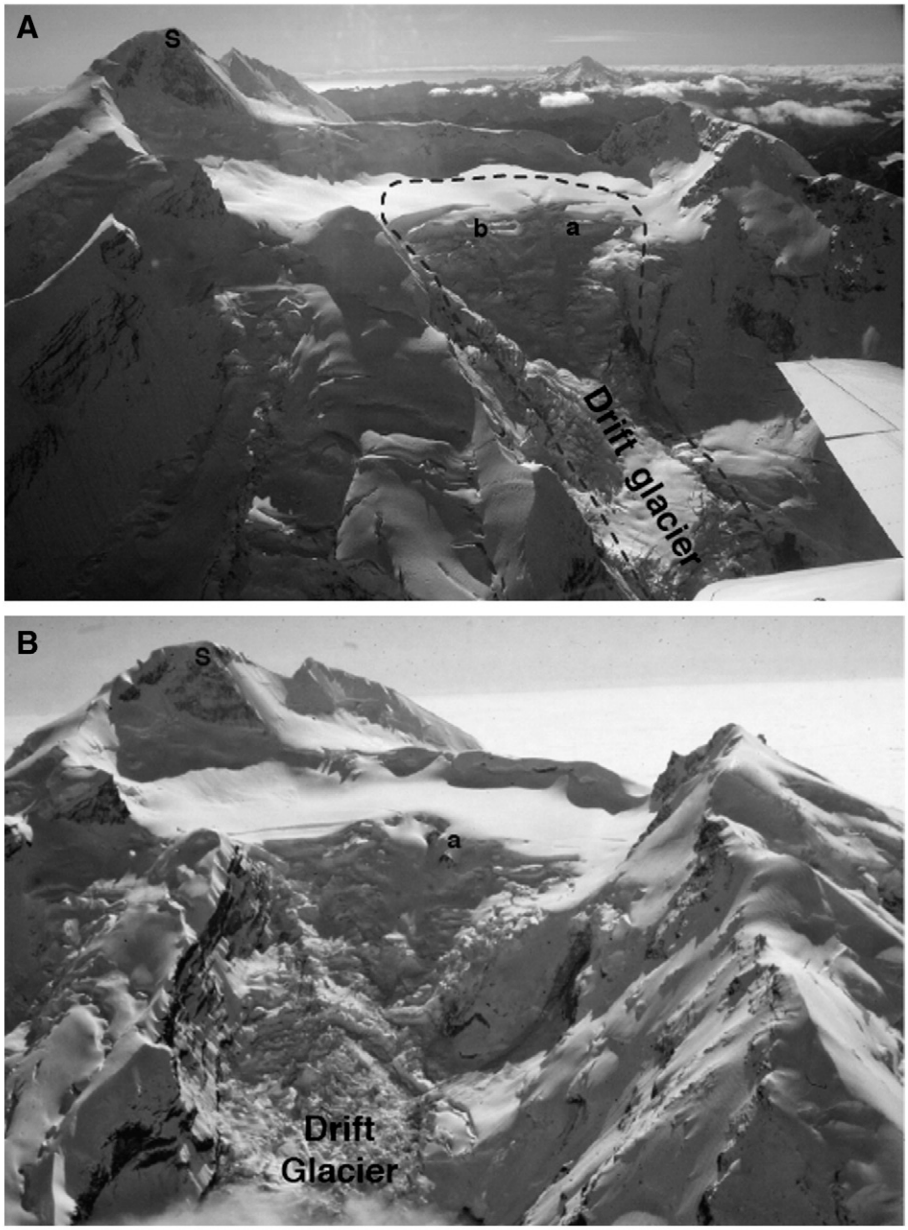

Fig. 2. A) Photograph of summit crater of Redoubt Volcano, September 16, 2007. The dashed line indicates the approximate area of ice loss resulting from the 2009 eruption. The total amount of ice removed by the eruption was about $1–2.5 \times 10^8$ m^3. Letter **a** locates the last dome emplaced during the 1966–68 eruption, and letter **b** locates the last dome emplaced during the 1989–90 eruption. Feature labeled **S** is the summit (3108 m). View is toward the southwest with Iliamna Volcano in background. Photograph by R.G. McGimsey, U.S. Geological Survey, Alaska Volcano Observatory. B) Photograph of summit crater of Redoubt Volcano, September, 1986. Letter **a** locates the last dome emplaced during the 1966–68 eruption. Feature labeled **S** is the summit (3108 m). View is toward the southwest. Photograph by D. Richter, U.S. Geological Survey.

slurry lahars, ice-diamict flows, and mixed avalanches) typically have volumes of 10^7 m^3 or less and runout distances up to about 15 km; such flows are relatively rare and require unique circumstances to develop (Pierson and Janda, 1994; Waitt et al., 1994; Cronin et al., 1996; Kilgour et al., 2010). Lahars more commonly consist of water-saturated, high-concentration mixtures of rock fragments, fine sediment, and only minor amounts of ice. Lahars at high-altitude or high-latitude volcanoes typically are initiated by the dynamic interaction of hot pyroclastic debris with snow and ice and occur frequently during explosive eruptions at snow- and ice-clad volcanoes (Major and Newhall, 1989; Walder, 2000a, 2000b). In contrast to ice-rich lahars, ice-poor lahars can have flow volumes as much as 10^8–10^9 m^3 and runout distances in excess of 100 km (Pierson et al., 1990; Mothes et al., 1998; Major et al., 2005).

1.3. Past lahars at Redoubt Volcano

Extensive inundation of the Drift River valley by large to very large[1] lahars is common during explosive magmatic eruptions of Redoubt Volcano. Valley-filling lahars were documented during the previous two eruptions in 1966–68 and 1989–90 (Sturm et al., 1986; Dorava and Meyer, 1994). On January 25, 1966, explosive activity generated a lahar of unknown volume (assumed to be large to very large) that inundated the lower Drift River valley (extent of inundation not known), transporting blocks of ice many meters in diameter

[1] "Large" lahars have near-source peak discharges of 10^3–10^4 m^3 s^{-1}; "very large" lahars have near-source peak discharges of 10^4–10^6 m^3 s^{-1} m^3 (Pierson, 1998). Corresponding volumes, modified from Jakob (2005), are roughly 10^6–10^7 m^3 for large lahars and 10^7–10^9 m^3 for very large lahars.

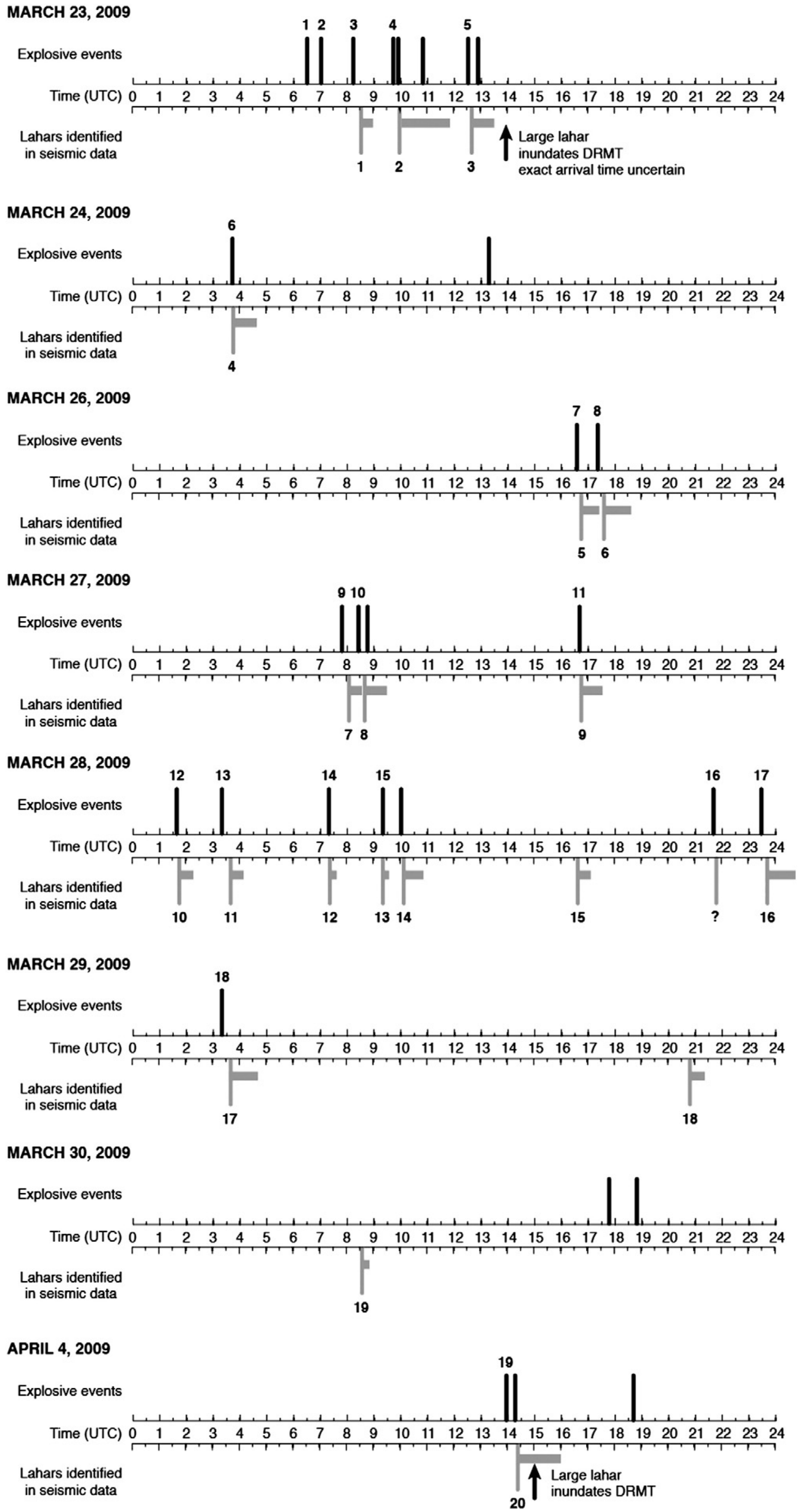
MARCH 23, 2009
Explosive events
1 2 3 4 5
Time (UTC) 0 1 2 3 4 5 6 7 8 9 10 11 12 13 14 15 16 17 18 19 20 21 22 23 24
Lahars identified in seismic data
1 2 3
Large lahar inundates DRMT exact arrival time uncertain
MARCH 24, 2009
Explosive events
6
Time (UTC) 0 1 2 3 4 5 6 7 8 9 10 11 12 13 14 15 16 17 18 19 20 21 22 23 24
Lahars identified in seismic data
4
MARCH 26, 2009
Explosive events
7 8
Time (UTC) 0 1 2 3 4 5 6 7 8 9 10 11 12 13 14 15 16 17 18 19 20 21 22 23 24
Lahars identified in seismic data
5 6
MARCH 27, 2009
Explosive events
9 10 11
Time (UTC) 0 1 2 3 4 5 6 7 8 9 10 11 12 13 14 15 16 17 18 19 20 21 22 23 24
Lahars identified in seismic data
7 8 9
MARCH 28, 2009
Explosive events
12 13 14 15 16 17
Time (UTC) 0 1 2 3 4 5 6 7 8 9 10 11 12 13 14 15 16 17 18 19 20 21 22 23 24
Lahars identified in seismic data
10 11 12 13 14 15 ? 16
MARCH 29, 2009
Explosive events
18
Time (UTC) 0 1 2 3 4 5 6 7 8 9 10 11 12 13 14 15 16 17 18 19 20 21 22 23 24
Lahars identified in seismic data
17 18
MARCH 30, 2009
Explosive events
Time (UTC) 0 1 2 3 4 5 6 7 8 9 10 11 12 13 14 15 16 17 18 19 20 21 22 23 24
Lahars identified in seismic data
19
APRIL 4, 2009
Explosive events
19
Time (UTC) 0 1 2 3 4 5 6 7 8 9 10 11 12 13 14 15 16 17 18 19 20 21 22 23 24
Lahars identified in seismic data
20
Large lahar inundates DRMT

Table 1
Estimates of ice loss[a] from the Drift glacier and the Drift River valley during 2009 eruption of Redoubt Volcano.

Time period	Estimated ice loss, in m^3	Meltwater volume[b], in m^3	Percent of total Drift glacier ice loss	Mechanism of ice removal and comments
July 31, 2008 to March 20, 2009	$3–7 \times 10^6$	$3–6 \times 10^6$	<1	Fumarolic emissions and associated melting, magmatic heat flux
March 20–26, 2009	$0.5–1.5 \times 10^8$	$0.5–1.5 \times 10^8$	5–15	Explosive eruptive activity, near vent pyroclastic flows. Includes lahars of March 23 and 26.
March 23, 2009	Unknown	Unknown	Unknown	Snow eroded and melted by lahars of March 23 in the Drift River valley
March 27–April 4, 2009	Unknown	Unknown	Unknown	Explosive eruptive activity, near vent pyroclastic flows
April 4, 2009	$0.5–1 \times 10^8$	$0.5–1 \times 10^8$	12	Explosive eruptive activity and pyroclastic flows that swept across parts of the Drift glacier
Totals	$1–2.5 \times 10^8$	$0.9–2.3 \times 10^8$	10–25	Pre-eruption ice volume of the Drift glacier about 1×10^9 m^3 (Trabant and Hawkins, 1997)

[a] Ice loss estimates made from analysis of satellite imagery where area of ice removal was measured in ArcMap. Ice thickness information from Trabant and Hawkins (1997). Reported values probably accurate to ±20%, largely because of uncertainties associated with estimating ice thickness.
[b] Determined by multiplying total ice loss value by 0.9.

and forcing the evacuation of a survey crew working in the area of the yet-to-be constructed DRMT (Anchorage Daily News, XIX, no. 149, 1966). A second lahar was generated on February 9, 1966, but apparently contained little or no ice (Riehle et al., 1981). Eyewitness accounts of the lahars indicated local flow depths of at least 4–6 m, but because no subsequent studies of the lahars were done, their volumes, peak discharges, and other details are unknown.

During the 1989–90 eruption at least 18 lahars were generated by vigorous vent explosions or pyroclastic flows associated with collapses of lava domes (Brantley, 1990). Three of these lahars were large enough to threaten or cause damage to the DRMT (Dorava and Meyer, 1994) on December 15, 1989, January 2, 1990, and February 15, 1990. The January 2 lahar was the largest of the 1989–90 eruption and commenced as a meltwater flood of about 25 million m^3 (Trabant et al., 1994; Dorava and Meyer, 1994), which then entrained tephra, pyroclastic debris, supraglacial debris, and alluvium to transform to a lahar having a volume on the order of 10^7–10^8 m^3 (Gardner et al., 1994). The estimated peak discharge for this lahar was 16,000–80,000 $m^3\,s^{-1}$ in the upper Drift River valley about 2.5 km downstream of the terminus of Drift glacier (Dorava and Meyer, 1994). The lahar transported ice blocks up to 8 m in diameter to Cook Inlet and inundated the Drift River valley to an extent comparable to that of the largest 2009 lahars.

2. Eruption effects on Drift glacier in 2009

The past three historical eruptions of Redoubt Volcano have all occurred from vents within the ice-filled summit crater and resulted in significant ice loss. Ice and snow as much as 100 m thick occupied the summit crater and upper Drift glacier prior to the 1989–90 eruption (Trabant and Hawkins, 1997). Comparison of photographs taken before the 1989–90 and 2009 eruptions (Fig. 2) suggests that a similar amount of ice was present in the summit crater and the upper Drift glacier before eruptive activity began in 2009. Occasional observations by Alaska Volcano Observatory scientists indicated that the ice removed from the summit crater and upper Drift glacier during the 1989–90 eruption regrew in about 10 years, similar to the rate of glacier regrowth following the eruption in 1966–68 (Sturm et al., 1986). Increased heat flow and fumarolic activity during the 8 months of precursory unrest prior to the 2009 eruption caused some melting of ice and the formation of collapse features by late February 2009 (Bleick et al., 2013). Our mapping of ice-melt features on satellite imagery, aerial observations, and estimates of ice thickness suggest that $3–7 \times 10^6$ m^3 of glacier ice and snow was lost from the crater and upper Drift glacier between late July 2008 and March 20, 2009.

At the time of the 2009 eruption, the upper part of Drift glacier occupied a narrow, steep, bedrock gorge downslope of the crater breach. The gorge not only restricted glacier width but also funneled pyroclastic flows and meltwater floods originating at the crater. Topographic focusing of hot flows within the gorge is a mechanism for enhancing ice scour and melting and appears to be a highly efficient process for meltwater generation.

At least 5 major vent-clearing explosions on March 23 (Schaefer, 2012; Bull and Buurman, 2013) removed glacier ice and snow, destroyed a small lava dome (and possibly all or most of the last 1990 lava dome), and produced a funnel-shaped explosion crater within the larger, ice-filled summit crater. Explosive events identified throughout the paper by numerals (Fig. 3) are the main, named events associated with explosion signals (Schaefer, 2012; Bull and Buurman, 2013). Reanalysis of seismic data identified several additional less vigorous explosive events, but these were not numbered sequentially. Proximal tephra deposits from explosive event 5, the last major explosive event on March 23 contained significant amounts of angular pebble-sized ice particles (Wallace et al., 2013) ejected from the vent area; melting probably contributed some water for lahar generation.

Aerial observations of the Drift glacier gorge area made on the afternoon of March 23, showed that the glacier had been locally scoured to bedrock. Although no pyroclastic-flow deposits were identified, the degree of ice erosion and the size of the ensuing lahar suggest that small but effective ice-melting pyroclastic flows may have formed. Meltwater generated by subglacial hydrothermal activity and stored in the summit crater beneath the Drift glacier also may have been released during the initial phase of the eruption on March 23. However, any water stored in the crater was probably of limited volume owing to geometric constraints and the prevalence of ice-collapse features indicating release, rather than storage, of meltwater. Another source of water for March 23 lahars was river ice and snow in the Drift River valley, where the snow depth was up to 2 m.

Analysis of a satellite image obtained on March 26, the first clear day after March 23, showed that about $0.5–1.5 \times 10^8$ m^3 of ice and snow had been removed from the upper Drift glacier, including part of the summit crater (Table 1). This value reflects the total ice loss caused by explosive events 1–8 (Fig. 3), much of the loss probably occurred during events 4–6, which were major eruptive events associated with significant lahars. Explosive events 9–18 from March 27–29

Fig. 3. Timeline of explosive events and lahars during the 2009 eruption. Black vertical bars indicate the time (UTC) of the main numbered explosive events of the eruption and the unnumbered black vertical bars indicate the minor explosive events identified during reanalysis of seismic data (Schaefer, 2012). The gray vertical bars indicate the approximate time that lahar signals are detected in seismic data at stations DFR and RDE and are numbered consecutively to indicate individual lahars. The gray horizontal bars associated with the numbered lahars indicate the average duration of seismic signal at stations DFR and RDE where the signal is at least twice the background level. Locations of stations are shown in Fig. 1. Alaska Daylight Time (AKDT) is −8 h from UTC.

Table 2
Large to moderate sized lahars of the 2009 eruption of Redoubt Volcano identified in seismic data and time-lapse camera images, March 24–30, 2009. [Evidence: S, seismic data; TL, time-lapse camera image; V, visual observation. km^2, square kilometers].

Lahar number	Date	Associated explosive event(s)	Evidence	Extent of inundation
4	March 24	6	S, TL	Northern part of the upper Drift River valley, unknown elsewhere
5, 6	March 26	7, 8	S, V	Upper and middle reaches of the Drift River valley, extent uncertain in lower reach; see Figs. 7 and 8. Estimated area of inundation 66 km^2.
7, 8	March 27	9, 10	S	Unknown
9	March 27	11	S, TL	Upper Drift River valley, unknown elsewhere; see Fig. 9
10	March 28	12	S, TL	Upper Drift River valley, unknown elsewhere
11, 12, 13, 14	March 28	13, 14, 15	S	Unknown, occurred at night
15	March 28	None	S, TL	Unknown, not associated with explosive event
16	March 28	17	S, TL	Unknown
17	March 29	18	S, TL	Extensive inundation of the upper Drift River valley, unknown elsewhere
18	March 29	None	S, TL	Minor inundation of the upper Drift River valley, not associated with explosive event
19	March 30	None	S	Unknown, not associated with explosive event

caused further melting of Drift glacier, but the extent of ice loss during this period could not be determined because clouds continuously obscured the volcano and much of the Drift River valley. A strong explosion and collapse of a growing lava dome at 13:58 UTC on April 4 (event 19) removed another $0.5–1.0 \times 10^8$ m^3 of ice from Drift glacier. Pyroclastic flows from the dome collapse caused significant scour of the glacier surface and initiated a very large lahar.

The total ice volume lost during 2009 and 1989–90 eruptions was of the same order of magnitude and in both eruptions most of the ice loss occurred on the upper Drift glacier between about 700 and 2000 m altitude. Ice loss during 2009 was about $1–2.5 \times 10^8$ m^3 or about 10–25% of the total glacier volume (Table 1). The amount of Drift glacier removed during the 1989–90 eruption was 2.9×10^8 $m^3 \pm 5\%$ (Trabant and Hawkins, 1997), or about 30% of the total.

3. 2009 eruption and lahars

Explosive events between March 23 and April 4 destroyed at least two lava domes, triggered four large to very large lahars in the Drift River valley—two on March 23, one on March 26, and one on April 4—and several smaller lahars between March 24 and March 30 (Fig. 3, Table 2). The four largest lahars inundated most of the upper and middle reaches of the Drift River valley and a broad area of its lower reach. The lahars of March 23 and April 4 inundated much of the DRMT and left behind 1–2-m-thick deposits of ice-rich mud, sand, trees, and other vegetal debris. The lahars mainly flowed around protective dikes at the DRMT and overtopped them in several places; operations at the facility were severely impacted, but the lahar inundation did not result in any oil spills.

Most of the lahars triggered by the 2009 eruption were recorded in seismic data from stations DFR and RDE along the Drift River valley (Fig. 1). No lahars were observed directly, but limited aerial observations and remote camera images provided confirmation of several lahars, usually within hours of emplacement. Lahar signals in seismic data appeared soon after individual explosive events as sustained seismic activity having broadly distributed energy spectra and gradually decreasing seismic coda (Fig. 4; Buurman et al., 2013). Throughout the eruption, the lahar onset was defined as the time of minimum signal-to-noise ratio (SNR) between the peak of an explosion signal and a sustained lahar signal. The end of a lahar was defined as the time when the SNR decreased to less than 2. Uncertainties about the character of the seismic source and the propagation path of seismic energy between lahar source and seismic station make it difficult to infer anything specific about the flow characteristics of lahars from seismic data.

3.1. Lahars of March 23

Eight explosions within 7 h on March 23 produced three seismically detectable lahars in the upper Drift River valley (Fig. 3), at least one of which reached the DRMT and flowed into Cook Inlet. The first lahar of the eruption (lahar 1) occurred just after midnight local time (08:40 UTC) March 23. The three lahars detected seismically during this initial period of explosive activity (lahars 1, 2, and 3) correlate with explosive events 3, 4, and 5, respectively. It is not known if any small lahars were produced during explosive events 1 and 2, but no flowage signals were detected at stations DFR and RDE immediately following these events. Lahars 1 and 2 occurred at night and were not observed.

Lahar 2 had the longest seismic duration (111 min at both stations DFR and RDE) and among the highest maximum seismic amplitudes of all lahars of the eruption (Fig. 5) suggesting a substantial, energetic flow. This lahar appears to have resulted from two closely spaced explosive events at 09:38 UTC and 09:48 UTC on March 23 (Fig. 3).

Lahar 3 was detected seismically at 12:38 UTC and had a seismic duration of about 47 min and the second largest maximum seismic amplitude of all of the lahars (Fig. 5). Oblique aerial photographs taken during a late afternoon reconnaissance flight on March 23 show a fresh but thinly snow-covered lahar deposit that is wider and more extensive in the upper valley than a subsequent crosscutting lahar deposit that had no snow cover (Fig. 6A). The snow-covered deposit probably was produced by lahar 2 and the deposit lacking snow cover by lahar 3. In the lower valley, the crosscutting

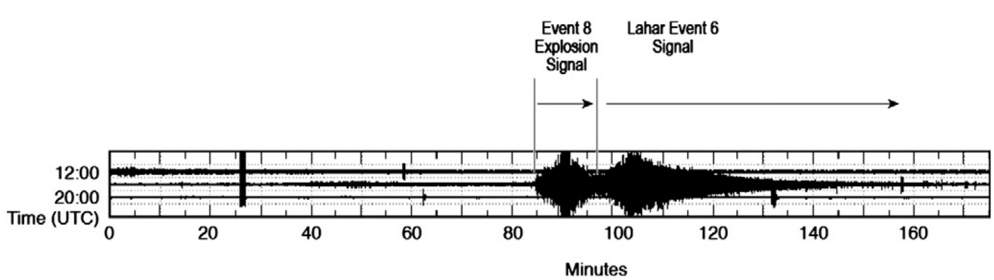

Fig. 4. Helicorder record from seismic station RDE showing explosion and lahar signal associated with explosive event 8 and lahar event 6 on March 26, 2009. The character of the lahar signal shown here was typical of the lahar signals detected at stations DFR and RDE throughout the eruption.

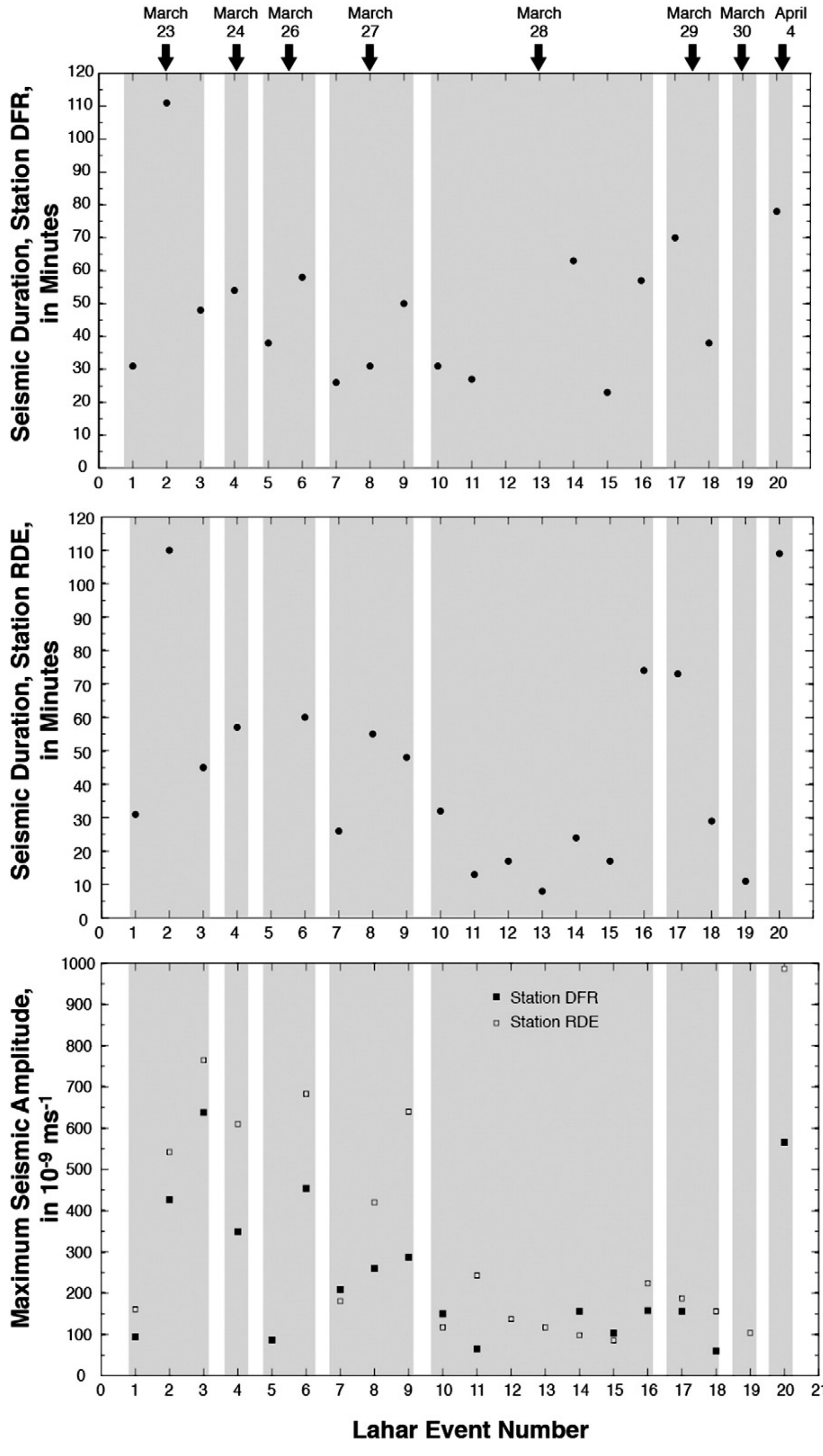

Fig. 5. Seismic duration and maximum seismic amplitude at stations DFR and RDE for lahar events of the 2009 eruption. The differences in seismic duration among stations primarily are a result of variable path effects and the degree of coupling between the flow and the bed. Shaded area indicates time period of 1 day. Locations of stations are shown in Fig. 1.

relations of these lahars were less distinct in aerial imagery and it was not possible to easily differentiate the extent of the two flows.

A lahar large enough to be noticed by DRMT personnel reached the facility between about 13:30 and 14:00 UTC (05:30–06:00 AKDT), and afterwards, all personnel were evacuated (Schaefer, 2012). If this was lahar 2, triggered by explosive event 4 at 09:38 UTC, its travel time would have been about 4–4.5 h and its average flow-front velocity (from summit crater vent to DRMT) would have been about 3 ms^{-1} (flow path length about 44 km). If the flow noticed at the DRMT was lahar 3, which was triggered by explosive event 5 at 12:30 UTC, its travel time would have been 1–1.5 h and the average flow-front velocity would have been about 8–12 ms^{-1}. Empirical travel time curves given in Pierson (1998) indicate that average travel times for large lahars to points 40 km from source are in the range of 1.5–3 h, and very large lahars are in the range of about 0.5–1.5 h. These values suggest that lahar 3 was the flow observed at the DRMT on the morning of March 23. We cannot confirm that lahar 2 did not reach as far as the DRMT; it likely did, but was not witnessed by personnel. The ice content of lahars 2 and 3 and the frozen ice and snow covered valley floor the lahars overrode likely resulted in unsteady, pulsatory flows. Ice jams forming at the front of lahar 2 could have slowed it enough to allow lahars 2 and 3 to merge.

The observations made during the March 23 reconnaissance flight indicated extensive lahar inundation throughout the Drift River valley (Fig. 6A), particularly in the area south of the DRMT in the Rust Slough–Cannery Creek drainage (Fig. 6B). The oil terminal had been surrounded and partly inundated by the lahar, and the runway at the facility was completely covered with sediment, ice, woody debris, and standing water. Along the middle and upper parts of the Drift River, trunks of mature trees were stripped of bark (probably by ice blocks entrained in the flow) to a height of several meters above the top of the lahar deposit and prominent mud and debris lines were evident along the channel (Fig. 6C). In many areas along the valley margin, deposits consisting chiefly of interlocking tabular ice blocks and subangular to rounded ice cobbles were emplaced and then frozen, preserving the ice-rich deposit fabric (Fig. 6D,E,F). Deposits consisting of an ice-grain matrix supporting cobble- to boulder-size clasts of ice (Fig. 6G) also were preserved in various locations throughout the valley. Two lahar deposits, possibly associated with lahars 2 and 3, were observed on March 31 at a location along upper Rust Slough near its confluence with the Drift River (Fig. 6H). The lower deposit was a massive ice-bearing, sandy hyperconcentrated-flow deposit and the upper deposit was similar to the ice-rich lahar deposits observed elsewhere in the Drift River valley.

The main channel of the Drift River along the northern side of the DRMT was plugged with sediment, ice, and logs, which caused the active channel to shift southward into the Rust Slough–Cannery Creek drainage (Fig. 7). Upstream in the confined 1.5–2-km-wide middle Drift River valley, prominent sediment benches, mud lines, and the upper limit of snow erosion indicated local flow depths of 6–8 m above the valley floor. At Dumbbell Hill, a bedrock knob in the Drift River channel about 3 km downstream of the Drift glacier terminus (Fig. 1), ripped up clasts of frozen sediment were emplaced on the upstream (west) side of the hill nearly reaching an equipment house on the top of the hill about 15 m above the valley floor. In this area, large clasts of ice, many meters in length, were scattered about on the valley floor. Unlike many of the 1989–90 lahar deposits, no steaming clasts or boulders of juvenile rock were observed on the surface of the March 23 deposit.

3.2. Lahars of March 24–30

At least 16 lahars were detected seismically, observed in time-lapse camera images, or both, from March 24–30 (Table 2, Fig. 3). Lahars on March 24–27 had seismic durations and amplitudes approaching or, exceeding those associated with lahars 2 and 3 on March 23 (Fig. 5). Lahar 6 on March 26 was one of the four largest lahars of the eruption based on relatively extensive inundation of the valley documented from satellite imagery and observations made during helicopter over flights (Figs. 8, 9). Most of the lahars that formed during this time period were probably water-rich hyperconcentrated to debris-flow lahars that had low peak discharges. Data and imagery obtained during this period provide the following observations:

(1) A pyroclastic flow associated with event 11 on March 27 reached the terminus of Drift glacier (travel distance about 9 km) about 3 min after the onset of explosive activity (average flow velocity about 50 $m s^{-1}$; Fig. 10B) and apparently triggered lahar 9. The time lag between the onset of explosive activity and the appearance of the lahar at Dumbbell Hill (13 km downstream of vent) were about 17 min (Fig. 10), but the timing and point of origin of the lahar are uncertain and we cannot meaningfully estimate lahar velocity. The lahar appears to have inundated part of the upper Drift River valley (Fig. 10B), but its downstream extent is not known.
(2) Some small lahars were not associated with seismically detected explosion signals (lahars 15, 18, 19; Fig. 3). These small lahars possibly were caused by release of meltwater from the glacier or local damming of channels on the glacier as also inferred in 1989–90 (Trabant et al., 1994).
(3) Some small lahars or floods were warm and their deposits steaming temporarily (Fig. 10B).
(4) Not all explosions generated seismically detectable floods or lahars (Fig. 3).

3.3. Lahar of April 4

Lahar 20 on April 4 was detected seismically, observed in time-lapse camera and satellite images, and was the most extensive lahar of the 2009 eruption. This lahar followed event 19 at 13:58 UTC, which involved a failure of the lava dome that had grown at the mouth of the summit crater. What appears to be the front of the April 4 lahar reaching Dumbbell Hill (13 km from the vent) was photographed by time-lapse camera at 14:11 UTC (Fig. 11), 13 min after explosive event 19 began. The lahar was detected for about 80 min at station DFR and about 1 h and 50 min at station RDE. This lahar had the largest maximum seismic amplitude of all lahars on station RDE and the second largest maximum seismic amplitude on station DFR, exceeded only by lahar 3 on March 23 (Fig. 5).

A reconnaissance flight on the afternoon of April 4 revealed that the lahar had completely inundated the upper and middle reaches of the Drift River valley and an extensive area of the unconfined lower reach of the valley including the DRMT (Figs. 12, 13). Inundation of the DRMT caused flooding of roads, and buildings, and again covered

Fig. 6. Photographs of March 23 lahar deposits. A) View downstream (east) from station DFR. Inundation limits from two flows are evident. The snow-covered deposit probably was emplaced during lahar 2, whereas the area free of snow is likely the deposit from lahar 3. Lahar 3 occurred about 2.5 h after lahar 2, and minor snowfall occurred prior to lahar 3. Photograph by R.G. McGimsey, U.S. Geological Survey, Alaska Volcano Observatory, March 23, 2009. B) Southwestern end of DRMT tank farm and protection levees showing minor lahar overflow of levees. Area of active flow is the Rust Slough–Cannery Creek drainage; flow direction is from right to left. Photograph by C. Read, U.S. Geological Survey, Alaska Volcano Observatory, March 23, 2009. C) View of the northern side of the Drift River channel showing maximum inundation limit of lahar 2 (arrows) and stranded ice blocks within deposits of lahar 3. The labeled ice blocks (IB) are 5–7 m in length; flow direction from left to right. Photograph by C. Read, U.S. Geological Survey, Alaska Volcano Observatory, March 23, 2009. D) Ice-rich lahar deposits consisting of tabular slabs of river and glacier ice exposed in cut bank along the Drift River. Photograph by C.F. Waythomas, U.S. Geological Survey, Alaska Volcano Observatory, April 17, 2009. E) Lahar deposits of 2009 eruption exposed along tributary to the Drift River south of Dumbbell Hill. Here, the March 23 deposits consist of an assemblage of subrounded to angular cobble- to boulder-sized clasts of ice, logs and other vegetation, in a matrix of crushed ice and frozen meltwater. Photograph by C.F. Waythomas, U.S. Geological Survey, Alaska Volcano Observatory, May 22, 2009. F) Ice-rich lahar deposits exposed along Rust Slough at the DRMT. These deposits consist of rounded to subangular, cobble to small boulder sized clasts of ice in a fine-grained granular ice matrix. Length of scale is 15 cm. Photograph by C.F. Waythomas, U.S. Geological Survey, Alaska Volcano Observatory, March 26, 2009. G) March 23 lahar deposit matrix and rounded clasts of glacier ice. Matrix material consists of rounded granules of ice and occasional lithic pebbles. Photograph by T.C. Pierson, U.S. Geological Survey, Cascades Volcano Observatory, May 22, 2009. H) March 23 lahar deposits exposed along upper Rust Slough near the confluence with the main stem of the Drift River. The stratigraphy revealed in this outcrop consists of Drift River alluvium at the bottom, pre-2009 eruption snow, sandy ice-bearing hyperconcentrated flow deposits, and ice-rich lahar deposits at the top. The March 23 lahar deposits exposed here were probably emplaced by lahars 2 and 3. Photograph by C.F. Waythomas, U.S. Geological Survey, Alaska Volcano Observatory, March 31, 2009.

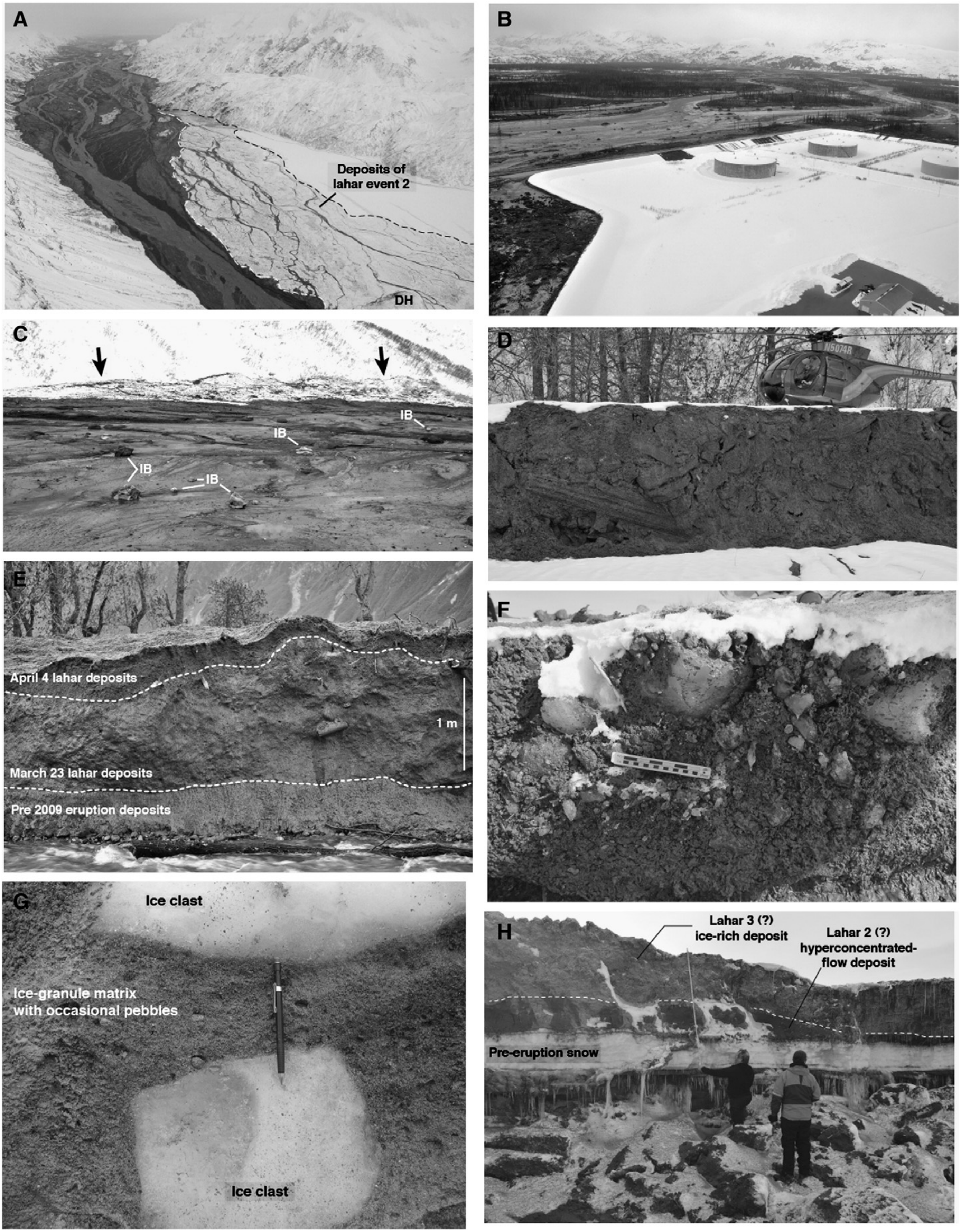
A
Deposits of
lahar event 2
DH
B
C
IB
IB
IB
IB
IB
D
E
April 4 lahar deposits
1 m
March 23 lahar deposits
Pre 2009 eruption deposits
F
G
Ice clast
Ice-granule matrix
with occasional pebbles
Ice clast
H
Lahar 3 (?)
ice-rich deposit
Lahar 2 (?)
hyperconcentrated-
flow deposit
Pre-eruption snow

the airstrip with muddy sediment, woody debris, blocks of ice, and other debris. The lahar surrounded the oil storage area and reached the top of, but did not breach, the tank containment levees. Minor flow and wet ground were observed along the main channel of the Drift River indicating that partial flow was reestablished temporarily in the main stem of the channel north of the DRMT. As the lahar waned, active flow was confined to distributary channels south of the DRMT (mainly Rust Slough) where it remained as of autumn 2011.

Although many blocks of glacier and river ice 2–5 m in length were observed on the surface of the April 4 lahar deposit as far downstream as the DRMT, internally the deposit was mostly devoid of ice. Some of the ice clasts probably were reworked from the March 23 deposit, but others were eroded from Drift glacier. The April 4 lahar formed ubiquitous deposits of gravel, sand, and mud that completely buried prior lahar deposits, including those emplaced on March 23.

4. Deposit characteristics of March 23 and April 4 lahars

The lahars that formed on March 23 and April 4 were the largest of the 2009 eruption, and deposits produced by these flows were preserved throughout the Drift River valley, especially along the valley margins (Fig. 14). No deposits attributed to other lahars were identified during field studies after April 4, suggesting that the April 4 flow either obscured or removed all evidence of them.

4.1. Characteristics of March 23 deposits

The maximum extent of the lahars emplaced on March 23 (Fig. 7) was mapped using oblique aerial photographs obtained during reconnaissance flights on March 23 and a composite aerial image of the lower Drift River valley obtained on March 31, 2009, by Aerometric, Inc. By the time the March 31 imagery was collected, the March 26 lahar had occurred and snow had fallen and covered parts of the deposit making it difficult to identify the limits of the lahar in some areas.

Except for one location, deposits of the three March 23 lahars could not be differentiated in outcrop. Aerial photographs of the upper Drift River valley show two apparent deposits (Fig. 6A), probably associated with lahars 2 and 3, but later field studies revealed only a single, undifferentiated deposit in downstream areas. Some outcrops may have been composites of the two deposits, but no internal boundaries were noted, except in one outcrop near the DRMT (Fig. 6H). At the location along upper Rust Slough, a 10–50 cm thick, massive, ice-bearing sandy deposit was observed overlying pre-eruption snow and ice; this deposit was overlain by an ice-rich lahar deposit (Fig. 6H). These two deposits could record inundation of the lower valley by lahars 2 and 3 and it appears that these deposits were emplaced by coarse-grained ice-laden slurries that froze solid soon after deposition. The March 23 deposit is underlain either by pre-eruption snowpack (corn snow with ice granules a few millimeters in diameter; Fig. 6H) or by fluvial deposits of the pre-eruption valley floor. In some outcrops, entrainment of the underlying snowpack was clearly indicated by irregular blocks of snow preserved within the lahar deposit as well as lenses and stringers of ice- and snow-rich laharic material that extend into underlying snow.

The March 23 lahar deposit was composed mostly of ice fragments, ranging from sand-size grains to much larger clasts of glacier and river ice. In some locations, the deposit was clast supported and consisted predominantly of equant blocks of glacier ice up to several meters in diameter and tabular slabs of river ice several meters in length (Fig. 6D). In other locations the deposit was matrix-supported with widely dispersed ice clasts (and some rock clasts) (Fig. 6E,F). Matrix material was composed of rounded grains of clear ice (Fig. 6G), estimated in the field to be largely in the range of 1–4 mm in diameter. Sand- to silt-size mineral grains, if present, were confined to the interstices between the framework ice grains and were frozen in the interstitial pore water. Rare cobble- to pebble-size, angular to subangular rock clasts in the deposit consist of dense, non-vesicular, phenocryst-rich andesite that were either fragments of older dome rock, fragments of new magma erupted during explosive events 4 and 5, or both. Rare rounded to subrounded rock clasts derived from the underlying alluvium were present locally, and the non-ice detritus also included logs and other vegetal debris. The volumetric content of rock fragments within the lahar deposit was estimated in the field to range between 5 and 20%. Measured bulk density for 9 matrix samples of the deposit averaged about 1.0 ± 0.1 gcm^{-3}.

The March 23 lahars inundated about 100 km^2 of the Drift River valley (Fig. 7). The maximum observed thickness was 5 m. Aerial observations indicated that mud lines on trees near the middle of the valley, where the lahar was flowing in a relatively straight channel, were locally as much as 2–4 m above the top of the lahar deposit. In other areas, lahar high-water marks were 6–8 m above the valley floor. Mud lines on buildings and trees at the DRMT indicate a distal flow depth of about 2 m. Because of poor weather and eruption hazards, it was not possible to make systematic measurements of high-water marks associated with the March 23 lahars.

4.2. Characteristics of April 4 deposit

The deposit of the April 4 lahar consisted almost entirely of massive to horizontally stratified, poorly sorted sand to fine gravel, up to 6 m thick where examined, and thickest in slack water areas along the valley margin (Fig. 15). In several outcrops near the valley axis in the upper Drift River valley, the deposit was a 1–2 m thick, massive, very poorly sorted, gray, pebble-to-cobble bearing diamict (Fig. 15B), suggesting that a component of the lahar had achieved debris-flow sediment concentrations prior to transformation to hyperconcentrated flow. The matrix of the April 4 deposit contained no obvious ice fragments. Rock material in the deposit consists mainly of cobble- to boulder-sized fragments of dense to slightly vesicular, locally prismatically jointed, medium- to light-gray juvenile andesite (Fig. 15A,B), which we infer to have been part of the lava dome destroyed during event 19 (Schaefer, 2012; Coombs et al., 2013). The April 4 deposit also contained subrounded blocks of glacier ice scoured from Drift glacier (some as large as 200–300 m^3) and some meter-sized tabular clasts of river ice, which probably were reworked from the March 23 deposits. These ice blocks were found throughout the Drift River valley, but in low amounts relative to the March 23 deposit. The stratified April 4 deposits locally exhibited water-escape structures and a capping deposit of silt, indicative of rapid deposition and low deposit permeability (Fig. 15D)—characteristics of deposition by hyperconcentrated flow (Pierson, 2005). A white precipitate coated many clasts on the surface of the deposit.

The extent of the April 4 lahar was mapped on a satellite image obtained on the afternoon of April 4 (Fig. 13). The color of the lahar deposit contrasted markedly with adjacent snow cover (Fig. 12), which permitted easy recognition and detailed mapping of the deposit. The April 4 lahar inundated an area of about 125 km^2, an area up to 20% greater than that inundated by the March 23 lahar, having a total extent that was partly obscured by snow. Field visits to the Drift River valley after April 4 allowed us to examine both lahar deposits, and to document high-water marks of the April 4 lahar left primarily as mud lines on trees. Generally, it was possible to measure the height of mud lines above the nearest active channel bed and above the nearest terrace surface to estimate local flow depths. These measurements are used below to estimate discharge and volume.

4.3. Comparison of matrix material

Samples of lahar matrix collected from both the March 23 ($n = 2$) and April 4 ($n = 17$) deposits were sieved to determine particle size distributions of material smaller than 4 mm. The April 4 deposit consists

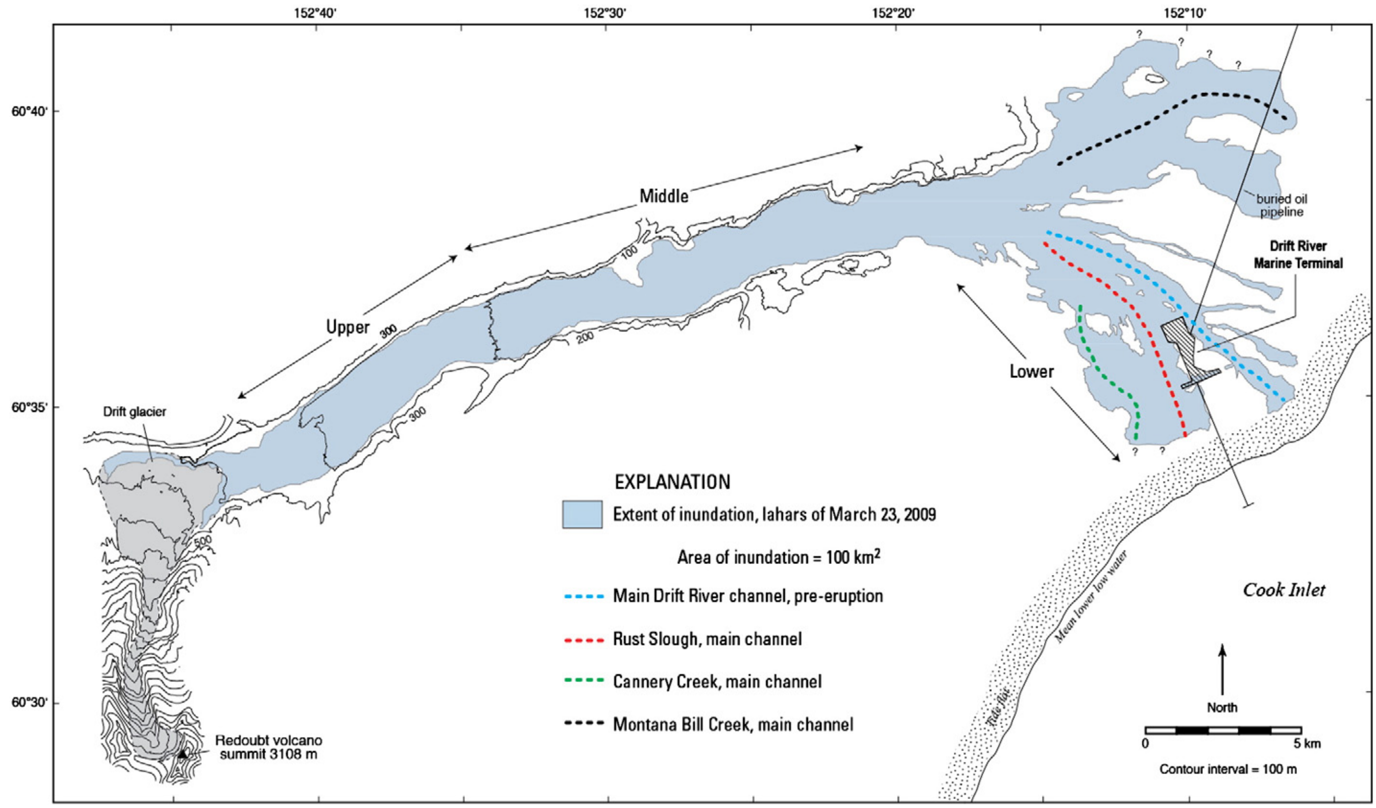

Fig. 7. Map of March 23, 2009 lahar deposit in the Drift River valley. Area of deposit mapped on composite aerial photograph obtained by Aerometric, Inc., March 31, 2009. Snow cover obscured parts of the deposit, so extent queried where uncertain.

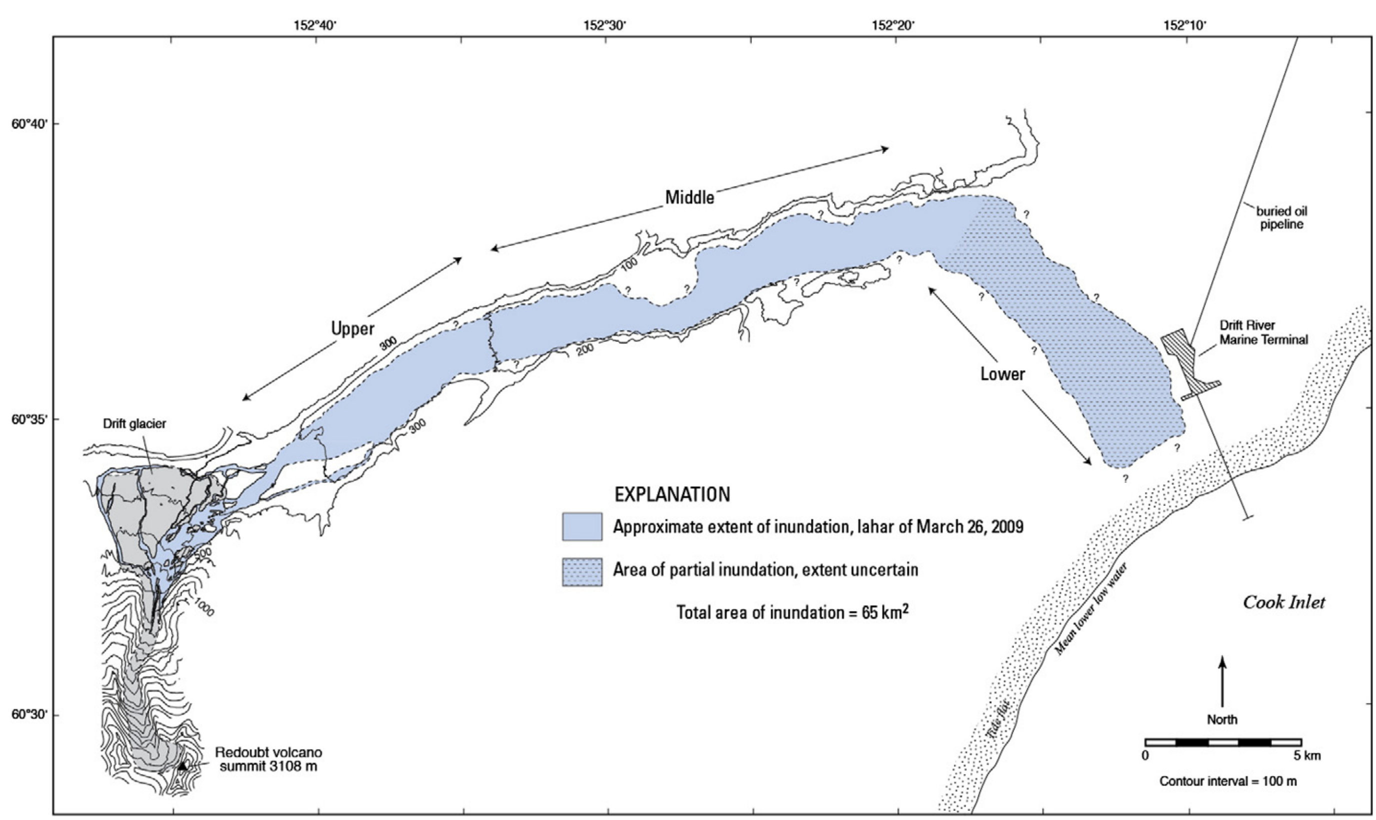

Fig. 8. Map of March 26, 2009 lahar deposit in the Drift River valley. Extent of deposit determined from satellite image of the upper Drift River valley and oblique aerial photographs acquired on March 26, 2009. Extent of deposit in the lower Drift River drainage uncertain.

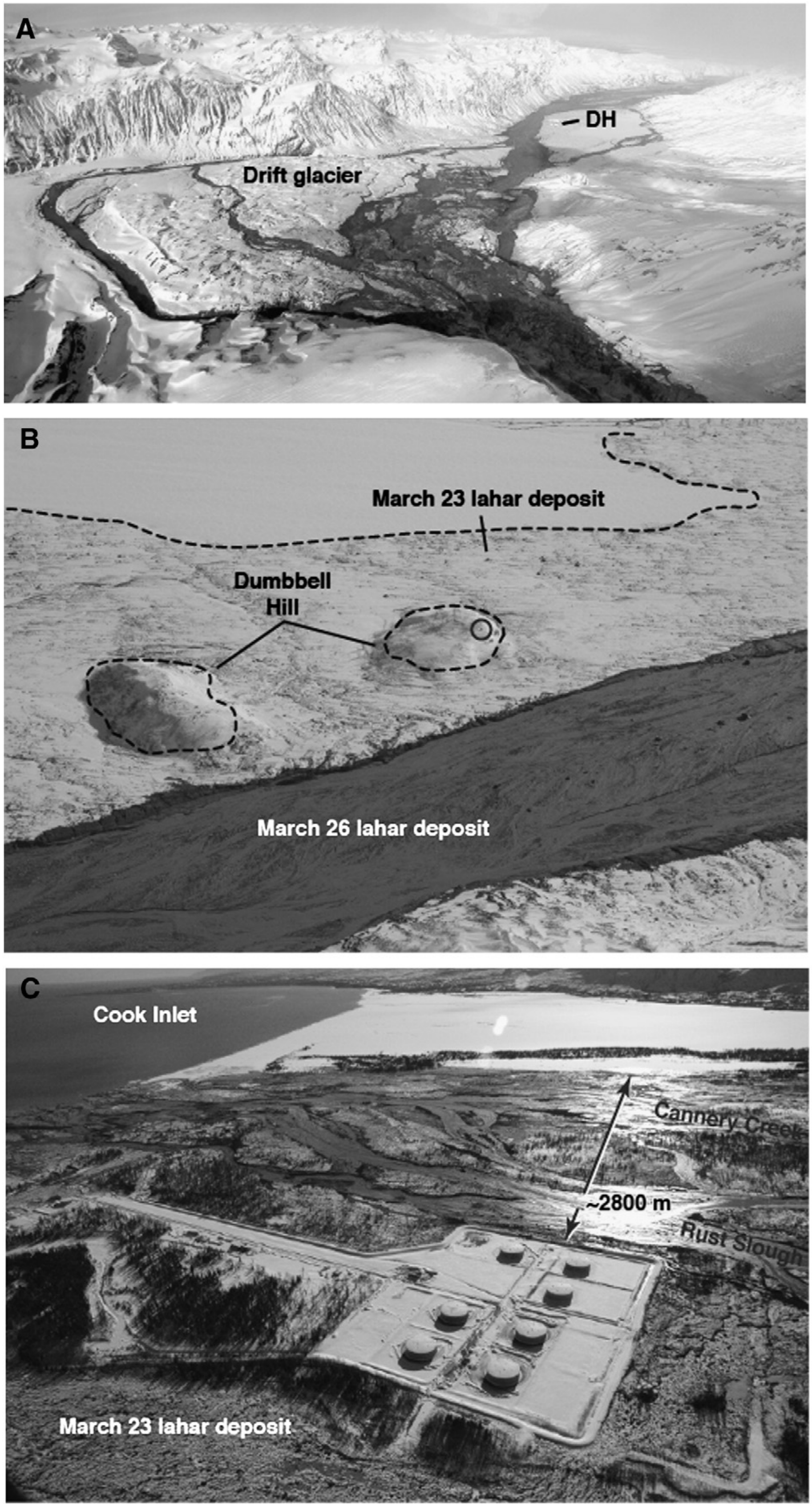

Fig. 9. Photographs of March 26 lahar deposits taken during reconnaissance flight, afternoon of March 26, 2009. A) Upper Drift River valley and piedmont lobe of Drift glacier showing extent of inundation (dark channels) associated with lahars 5 and 6. DH shows location of Dumbbell Hill. B) Dumbbell Hill area showing extent of lahars of March 23 and 26. Circle on upstream (west) part of Dumbbell Hill locates instrument house containing time-lapse camera. Flow direction is from right to left. C) Lower Drift River valley looking south from DRMT. Flow from the lahars of March 26 was confined to the Rust Slough–Cannery Creek drainage where the flow width was about 2800 m. Peak flow depth in this area was about 1 m. No flow entered the main channel of the Drift River (foreground), which remained blocked by deposits of the March 23 lahars. All photographs by C.F. Waythomas, U.S. Geological Survey, Alaska Volcano Observatory.

Fig. 10. Time-lapse camera images from Dumbbell Hill of pyroclastic flow and lahar associated with eruptive event 11 and lahar 9. View is toward the west and valley width in field of view about 2 km. A) Pyroclastic flow emerging from the Drift glacier gorge and extending from left to right across piedmont lobe of the Drift glacier. Minor snowfall occurred after image was taken. B) Fresh, steaming, lahar deposits in the upper Drift River valley (shown by arrows).

mainly of fine-skewed, poorly sorted, fine-to-coarse sand, whereas the two March 23 samples are slightly coarser and less well sorted (Fig. 16). A sample collected from the distal northern margin of the April 4 deposit (sample R, Fig. 17) consists of about 90% silt and finer material and probably records tranquil standing water conditions at this location. The April 4 deposit shows only minor variation and no apparent spatial trend in sand and silt content, sorting, and mean grain diameter (Fig. 17). Although we recognized gravel-rich debris-flow lahar deposits within 1–2 km of the terminus of Drift glacier, most of the April 4 lahar appears to have undergone minimal flow transformation after its initial transformation from debris flow to hyperconcentrated flow.

5. Discharge and volume estimates

Information about the hydraulic characteristics of the 2009 lahars was derived from field observations, analysis of satellite images, and indirect measurements of flow depth, runup, and width, and estimates of flow velocity. We have limited information about the flow characteristics of the March 23 lahar and thus provide only a generalized estimate of discharge for the upper part of the valley. The discharge and volume estimates for the April 4 event are better constrained, but still approximate because of uncertainties associated with determining flow depth, width, and velocity. All of the discharge and volume estimates include substantial uncertainty.

5.1. Peak discharge of March 23 lahar

We were unable to document flow depths directly for any of the first three lahars of the eruption. Aerial observations and photographs of the Dumbbell Hill area obtained after emplacement of the March 23 lahars indicate that the largest flow had a maximum width of about 2000 m (Figs. 6A, 7, 9B) and associated high-water marks approximately 6–8 m above the valley floor. The average flow depth in the Dumbbell Hill area may have been in the range of 2–4 m, but we were unable to confirm this. Cross-sectional areas inundated by the largest of these lahars probably were on the order of 4000–8000 m^2. Lahar runup on the upstream end of Dumbbell Hill was estimated in the field to be about 13 m above the channel floor, indicating an approximate flow velocity of 16 ms^{-1} (estimated

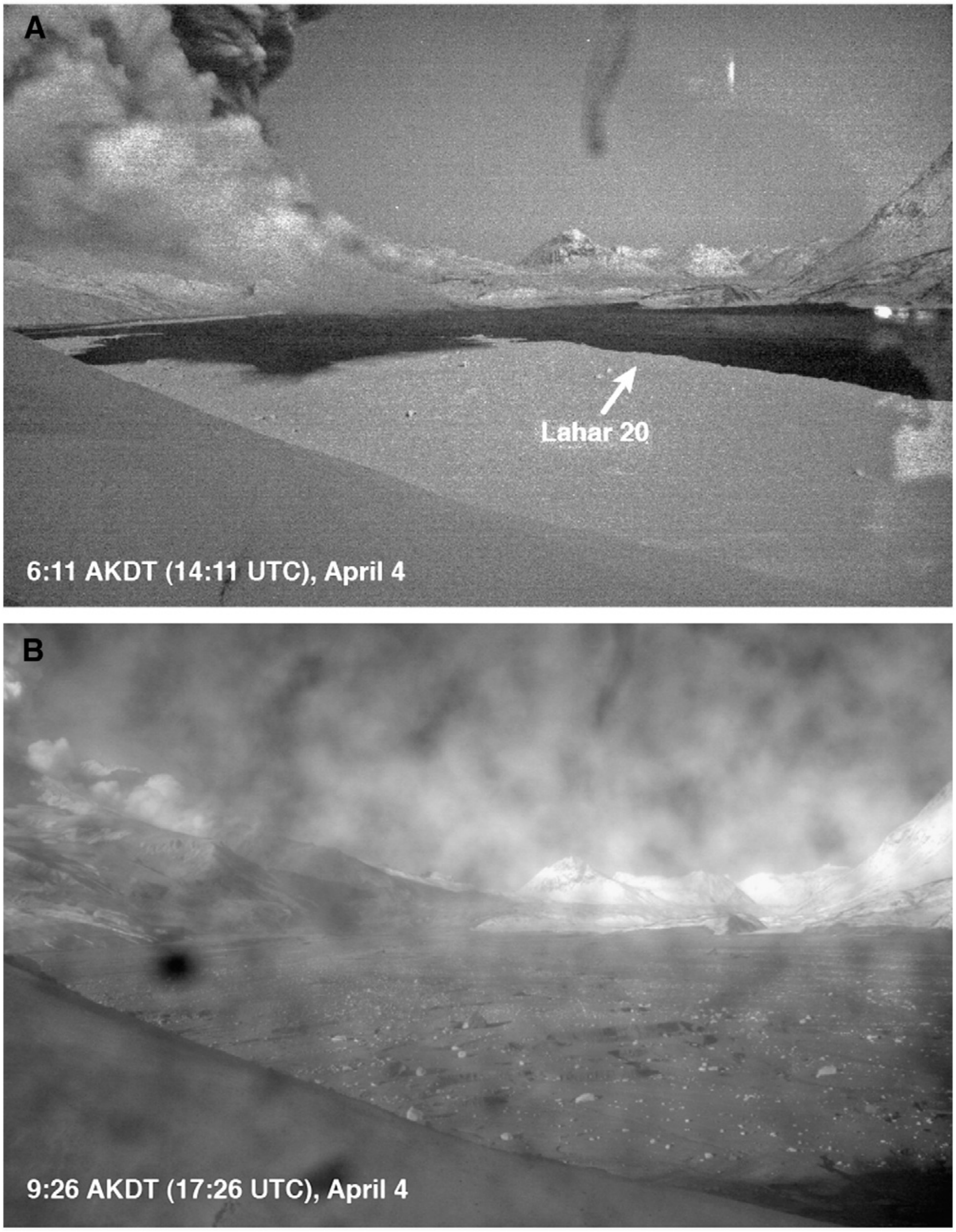

Fig. 11. Time-lapse camera images from Dumbbell Hill of lahar inundating the upper Drift River valley on April 4, 2009. View is toward the west and valley width in field of view about 2 km. A) Initial surge of water at the beginning of lahar 20, 13 min after the start of explosive event 19. Note eruption column in upper left of image. B) Extent of inundation of the upper Drift River valley associated with lahar 20 about 3 h after the lahar swept by Dumbbell Hill. Field of view partially obscured by ash on camera housing.

from the flow runup equation). Application of the runup equation assumes steady, uniform flow, which was unlikely for these ice-laden lahars. Debris flow velocity estimates made with this equation may be too high by 30% or more (Iverson et al., 1994). Furthermore, the ice-choked character of the flow may have created ice-shove, jamming, and other impediments. Smaller lahars in 1989–90 had measured flow velocities of 6–16 ms^{-1} in the upper valley (Dorava and Meyer, 1994). Thus, we use a range of values from 5 to 15 ms^{-1} for flow velocity. This suggests a peak discharge near Dumbbell Hill in the range of 20,000–120,000 $m^3 s^{-1}$ (or 10^4–10^5 $m^3 s^{-1}$).

5.2. Peak discharge of April 4 lahar

Flow depth, width, and velocity at the time of peak discharge for the April 4 lahar were estimated both from field evidence and from data on hyperconcentrated-flow lahars in the literature. Flow depth was estimated by measuring the height of mud coatings (mud lines) on trees above nearby deposit surfaces and above nearby active channel beds. These values provide a possible range of flow depths at the time of peak discharge, but because the bed may have aggraded during the flow and perhaps incised during waning flow, it is not possible to know where the bed was when the flow coated the trees. At some field locations, flow depths estimated from the height of mud lines above April 4 lahar terraces ranged from 0.4 to 5 m, with one site showing a local depth of about 6 m (Fig. 18B). Flow depths estimated from the heights of mud lines above the valley floor ranged from 1.4 to 13 m (Fig. 13). Maximum flow width normal to the flow path was scaled from satellite images, although in the lower reach it is unlikely that flow occupied all channels simultaneously. Flow velocities could not be indirectly estimated in the field for this lahar, so we used lahar velocity data from the 1989–90 lahars in Dorava and Meyer (1994).

Channel cross sections (Fig. 19) were derived from a 10-m DEM of the Drift River valley made from August 1990 topographic data

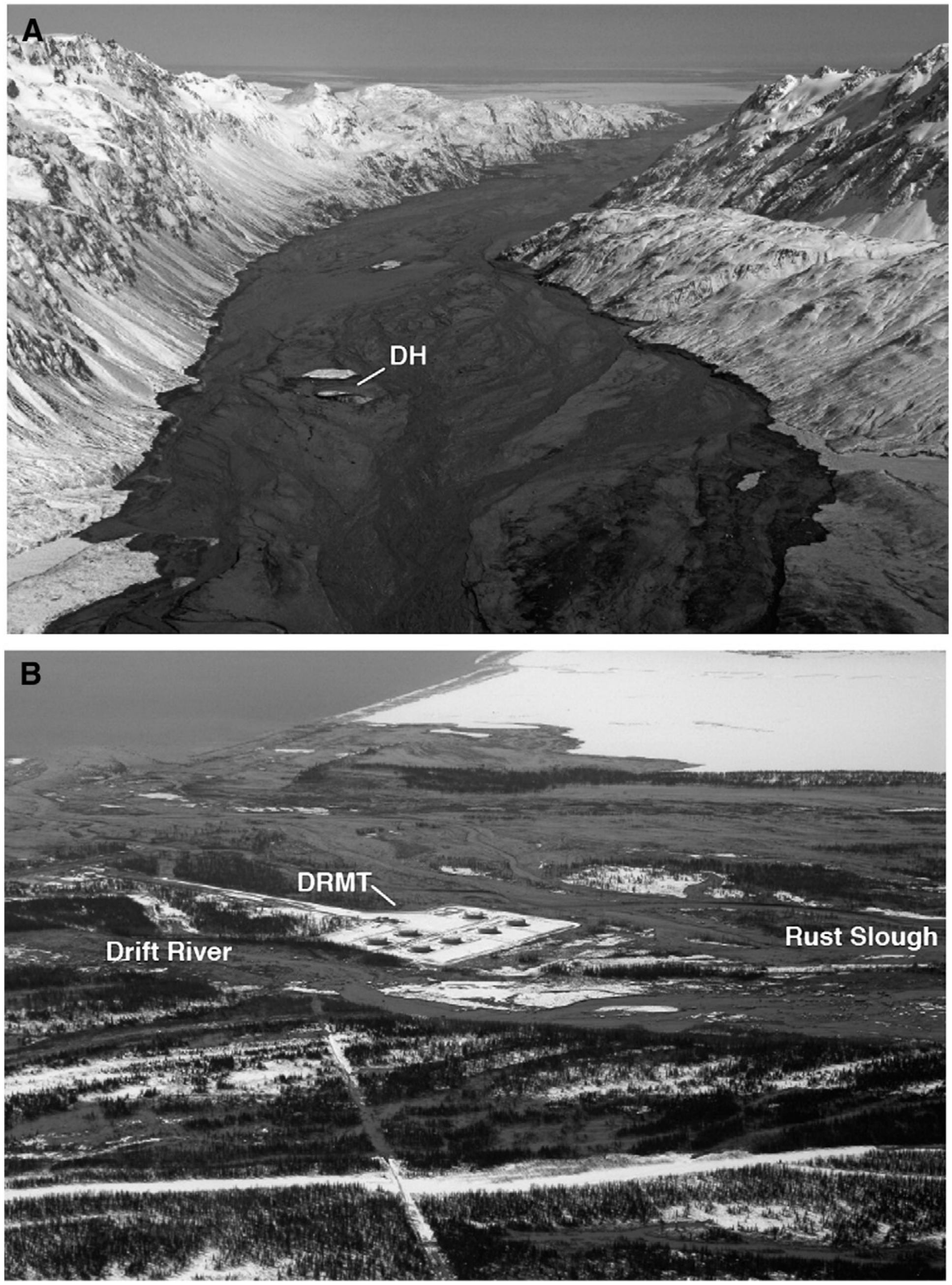

Fig. 12. Inundation of the Drift River valley associated with the lahar of April 4, 2009. A) View downstream (east) of the upper Drift River in the vicinity of Dumbbell Hill (DH). The width of the channel inundated by the April 4 lahar at Dumbbell Hill is about 2 km. Flow runup on the upstream end of Dumbbell Hill about 13 m. Photograph by C.F. Waythomas, U.S. Geological Survey, Alaska Volcano Observatory, April 4, 2009. B) Extent of inundation along the lower Drift River valley in the vicinity of the DRMT. View is toward the southwest. Photograph by C.F. Waythomas, U.S. Geological Survey, Alaska Volcano Observatory.

acquired by U.S. Geological Survey. The cross sections give approximate channel dimensions and are broadly representative of the channel shape at the time of the 2009 lahars, possibly to within several meters. We have no way to independently verify the pre-lahar channel geometry and were unable to obtain topographic data of the valley after the eruption ended. The April 4 lahar flowed over a valley floor that had been inundated by 18 previous lahars, including the extensive lahars of March 23 and 26. The valley floor was covered with a fill of sand, gravel, and slabs of ice from these events and intervening streamflow; some of this material was frozen. The degree of dissection of the valley floor is not known, but observations made on March 26 and 31 indicated that flows subsequent to March 23 had eroded parts of the valley floor, particularly along the main channel of the Drift River.

In the lower part of the valley at cross-section 4, west of the DRMT (Fig. 13), we assume that at least half and perhaps the entire cross section was occupied by flow at the peak stage of the April 4 lahar. A satellite image and oblique aerial photographs (Figs. 12B, 13) obtained on the afternoon of April 4 indicate that the entire cross section had been inundated and the maximum inundation width was about 3300 m. The height of mud lines above nearby active channel beds near cross-section 4 ranged from 1.5 to 4 m (Fig. 13) and the average flow depth is estimated at 2 m. High sediment-concentration water floods and hyperconcentrated-flow lahars may undergo rapid lateral channel migrations (e.g., Scott et al., 1996), so the flow may have been dispersed among multiple braided channels with intervening bars and islands. Average flow velocity of the January 2, 1990, lahar in the lower Drift River valley was perhaps as large as 4 ms^{-1}

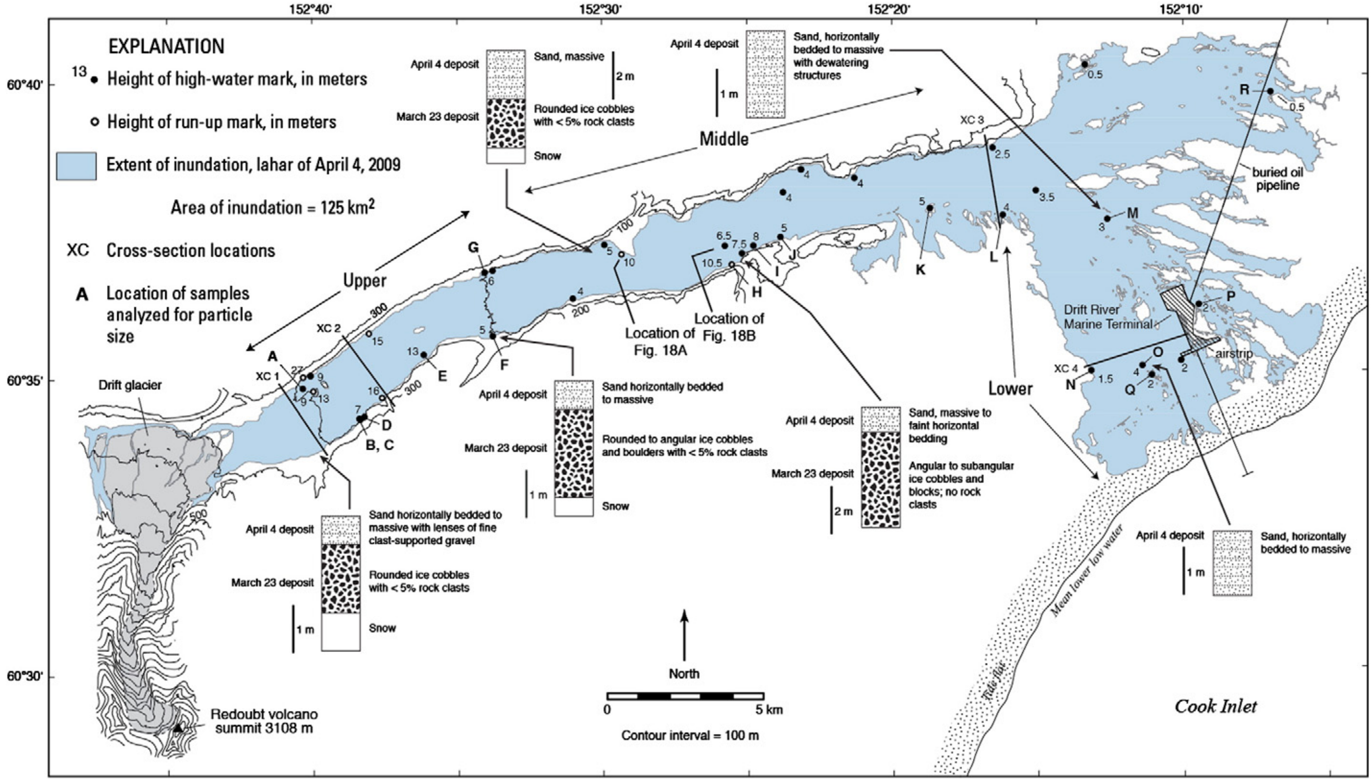

Fig. 13. Map of lahar inundation associated with lahar 20 on April 4, 2009. Local flow depths (closed circles) and flow run up (open circles) as determined by laser rangefinder measurements of high-water marks and mud lines on trees also are shown. Location of channel cross sections used for discharge estimates, and generalized stratigraphic profiles also are shown. Locations of samples analyzed for particle-size distribution are indicated by letters A–R.

(Dorava and Meyer, 1994), and comparable hyperconcentrated flows at a similar distance from their sources have had flow velocities of 2–4 ms^{-1} (Pierson, 2005). Thus, we use average flow velocities of 1 and 5 ms^{-1} to estimate possible discharges of the lahar in the lower part of the Drift River valley (Table 3). A reasonable range of peak discharges for a lahar occupying all of cross-section 4, with an average depth of 2 m, is 6000–33,000 $m^3\,s^{-1}$. If only one half of cross-section 4 was inundated at the peak stage of the lahar, the range of discharges would be 3200–16,000 $m^3\,s^{-1}$ (Table 3). Thus, an order-of-magnitude estimate of peak discharge for the April 4 lahar at the DRMT is about 10^3–10^4 $m^3\,s^{-1}$.

Peak discharge in the upper reach of the Drift River is less constrained. However, an order-of-magnitude estimate can be posited for cross section 1, on the basis of known flow width (Fig. 13), indirect measurements of the 1989–90 lahar velocities (3–23 ms^{-1}; Dorava and Meyer, 1994), and two indirect calculations of velocity along the main axis of the April 4 flow, based on flow runup on Dumbbell Hill and the adjacent north valley wall (16 and 23 ms^{-1}). The elevation of high-water marks measured in the area of cross-section 1 (Fig. 13) averaged about 8 m above the May 2009 valley floor, but we are not confident that this is a reasonable value for average flow depth. If the channel floor was aggrading during the peak stage of the flow, the average depth would have been less than this value, and if the channel was incising, it might have been locally greater. In addition, irregularities in the surface of the flowing lahar can produce high-water marks not representative of average depth. Thus, we infer an average flow depth in the range of 2–5 m. Our best estimates of the hydraulic variables are a flow width of 2100 m (assuming all of valley width was occupied), average depth of 2–5 m (thinner on margins, deeper along flow axis), and an average flow velocity of 10–15 ms^{-1}. These values give a range in peak discharge of 42,000–157,000 $m^3\,s^{-1}$, or 10^4–10^5 $m^3\,s^{-1}$, values that are roughly the same order of magnitude as those estimated for 1990 lahars (12,000–80,000 $m^3\,s^{-1}$; Dorava and Meyer, 1994). The discharge estimates for the 1990 lahars were made using slope-conveyance and slope-area techniques, both of which assume steady, uniform flow (Dorava and Meyer, 1994). Although these techniques generally are not applicable to lahars, they provide order of magnitude estimates of flow discharge.

5.3. Lahar volume estimates

Estimates of lahar volumes were obtained for the March 23 and April 4 lahars in two ways: (1) by multiplying deposit area by estimated average deposit thickness; and (2) by converting ice-loss volumes (see Section 2) to water equivalence, and then multiplying by a sediment (or ice) bulking factor to achieve the solids concentrations inferred from deposit sedimentology. Considerable error is inherent in both methods, given the available data and the high degree of uncertainty in assumptions of various factors such as cross-sectional area inundated by the lahars, average deposit thickness, and amount of ice loss that provided water to mobilize lahars. For the first method, inundation areas digitized from aerial photos and satellite imagery are among the best-constrained factors, at least for lahars of March 23 and April 4. Estimates of deposit thickness are based on scattered observations throughout the valley, many of which come from the valley margins. For the second method, ice-loss estimates discussed in Section 2 areas were converted to water equivalents, and for the April 4 lahar, this value was multiplied by a sediment-bulking factor (Scott, 1988), which was inferred from deposit textures (Table 4).

Within the uncertainties of the methods used, estimates of the volumes of the largest lahars of the 2009 eruption range from 10^7 to 10^8 m^3 (Table 4). The combined volume of lahars 2 and 3 on March 23 is estimated to range from $2–20\times10^7$ m^3, so the volume of each individual lahar must have been on the order of 10^7–10^8 m^3. The March 26 lahar had a volume of about 10^7 m^3 estimated on the basis

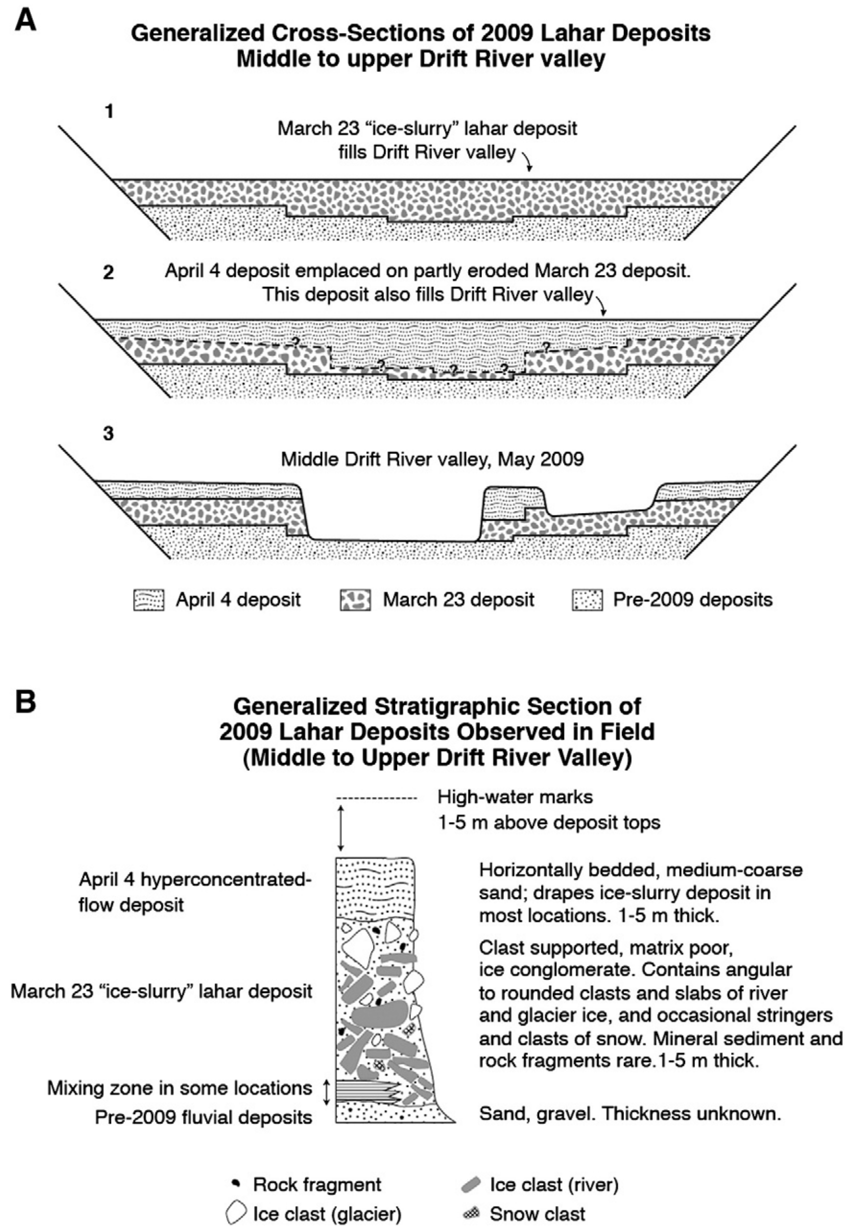

Fig. 14. Generalized cross-sections (A) and stratigraphy (B) of 2009 lahar deposits in the upper to middle Drift River valley.

of an area-average deposit thickness calculation (average deposit thickness = 0.2–1 m). The volume of the April 4 lahar is estimated to fall within the range of $6–25\times10^7$ m^3. The estimated peak discharges and volumes are consistent with published correlations of peak discharge to flow volume for debris-flow lahars and nonvolcanic debris flows (Mizuyama et al., 1992; Rickenmann, 1999; Jakob, 2005). Lahars 2 and 3 on March 23 and the dominantly hyperconcentrated-flow lahar on April 4 all appear to have had volumes of about the same order of magnitude as the largest lahar of the 1989–90 eruption on January 2, 1990 (Gardner et al., 1994).

6. Discussion

The lahars produced early in the 2009 eruption on March 23 were strikingly different in composition and flow type from the similarly sized April 4 lahar emplaced at the end of the explosive phase of the eruption. The March 23 flows were voluminous, water-saturated, granular mass flows composed predominantly of ice fragments that probably behaved as ice slurries. Smaller ice-rich mass flows with varying water contents have been previously described having been triggered by (a) liquid water explosively ejected out of crater lakes onto snowfields (Cronin et al., 1996; Lube et al., 2009; Kilgour et al., 2010); and (b) loading of snow slopes with explosively ejected ballistics or pyroclastic flows (Waitt et al., 1983, 1994; Pierson et al., 1990; Pierson and Janda, 1994). The ice-slurry lahars emplaced on March 23 were at least several times larger and traveled tens of kilometers farther than previously described ice-rich lahars. A key factor in the development of the ice-rich lahars on March 23 was the availability of snow and ice—Drift glacier at full volume and extensive, thick snowpack and river ice (as much as 2 m) in the Drift River valley. Outcrops of the March 23 ice-rich lahar deposit showed no apparent systematic downstream changes in internal structure and the deposit was consistently a massive ice-rich diamict. In contrast, the April 4 lahar contained only small amounts of ice some of which was eroded from the Drift glacier and some reworked from the March 23 deposits. The April 4 flow began as a debris-flow

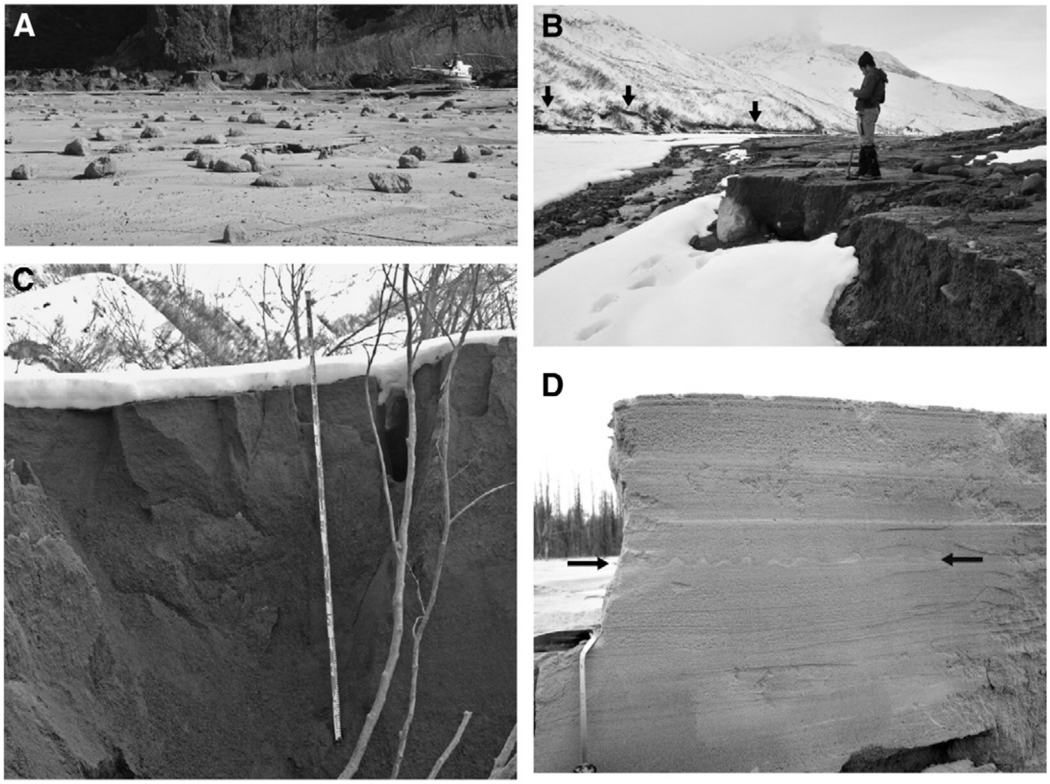

Fig. 15. Photographs of April 4 lahar deposits. A) Lahar deposits in middle reach of the Drift River valley showing clasts of juvenile andesite on deposit surface that were part of the lava dome that failed on April 4. Photograph by C.F. Waythomas, U.S. Geological Survey, Alaska Volcano Observatory. B) Upper reach of the Drift River valley with Redoubt Volcano in background. Person standing on cobble and boulder gravel lahar deposits near channel axis. Arrows indicate high water mark of April 4 lahar along the southern side of valley. Photograph by C.F. Waythomas, U.S. Geological Survey, Alaska Volcano Observatory. C) Massive-to-faintly-stratified sand deposits that are characteristic of the April 4 lahar deposit. Scale in photograph is 2 m in length. Photograph by C.F. Waythomas, U.S. Geological Survey, Alaska Volcano Observatory. D) Subhorizontally stratified fine-to-medium sand deposit exposed along the lower reach of the Drift River north of the DRMT. Convolute bedding shown by arrows suggests rapid loading of water-saturated beds. Trenching tool in lower left for scale. Photograph by T.C. Pierson, U.S. Geological Survey, Cascades Volcano Observatory.

lahar but quickly transformed to a more dilute hyperconcentrated-flow lahar.

Recent historical eruptions of Redoubt Volcano have all been characterized by vent clearing explosive activity followed by episodic dome growth and destruction (Miller, 1994), which led to extensive lahars and flooding in the Drift River valley (Sturm et al., 1986; Dorava and Meyer, 1994). Failures of large lava domes that grew in the summit crater have produced pyroclastic flows and voluminous lahars. Failure of the largest lava domes of the 1989–90 eruption produced substantial lahars on January 2 (dome volume about 3×10^7 m^3) and February 15, 1990 (dome volume about 1.5×10^7 m^3) (Miller, 1994; Dorava and Meyer, 1994). Event 19 on April 4, 2009, also was accompanied by a dome failure, which led to the largest lahar of the 2009 eruption. Although the exact volume of the dome that failed on April 4 is not known, it may have been as large as 3.6×10^7 m^3 (Bull and Buurman, 2013), similar to the volume of the lava dome that failed on January 2, 1990. On the basis of approximate volumes of failed domes and estimated volumes of lahars, it appears that eruptions of Redoubt Volcano involving failures of lava domes having volumes of about 10^7 m^3 tend to produce lahars having volumes in the range of 10^7–10^8 m^3.

Although it is clear that swift melting of glacier ice by pyroclastic flows created by dome collapse led to formation of the lahar on April 4, 2009, the mechanism of water generation associated with the March 23, 2009, lahar is less obvious. Because the lahars emplaced on March 23 were composed almost entirely of ice fragments, and because none of the rare volcanic rock fragments in the deposit was obviously juvenile, evidence for pyroclastic flow involvement in meltwater generation is weak. However, proximal tephra deposits associated with event 5 contained angular, pebble-sized ice clasts as well as dense to vesicular juvenile fragments (majority) and non-juvenile lithic clasts (Wallace et al., 2013), indicating that ice, pre-existing rock, and juvenile magma were explosively fragmented and ejected from the ice-filled summit crater. It is possible that explosive activity in the summit crater generated some meltwater by thermal and mechanical interaction with snow and ice around the vent. It also is possible that some water was ejected along with ice fragments from the crater. Such water may have accumulated beneath or within the summit crater ice as a result of fumarolic heating, and some may have come from water-saturated rock around the vent. It is also possible that a small dome may have grown in the vent during the nearly 3-hour interval between explosive events 4 and 5. If so, and if it grew at the maximum extrusion rate estimated for the 2009 eruption (35 m^3 s^{-1}, Diefenbach et al., 2013), then a modest-sized lava dome of about 3–4×10^5 m^3 could have been present. If such a dome had failed and rapidly fragmented, then a pyroclastic flow traveling a short distance over the upper Drift glacier could have produced some meltwater. The eruption columns generated during explosive events 4 and 5 reached about 14–18 km above sea level and were among the largest of the eruption sequence. A limited run-out pyroclastic flow possibly could have formed locally around the base of the eruption column and been funneled down the upper Drift glacier resulting in melting that led to the March 23 lahar. However, no pyroclastic-flow deposits were observed in the field, although it is unlikely that they would have been easily differentiated from thick tephra deposits high on the flanks of the volcano. Substantial ice was lost from the Drift glacier from March 20–26, and most of the ice loss likely was during the explosive events that triggered the lahars of March 23.

Large flows composed of ice and water often result from the release of ice jams that occur during the breakup of winter ice cover

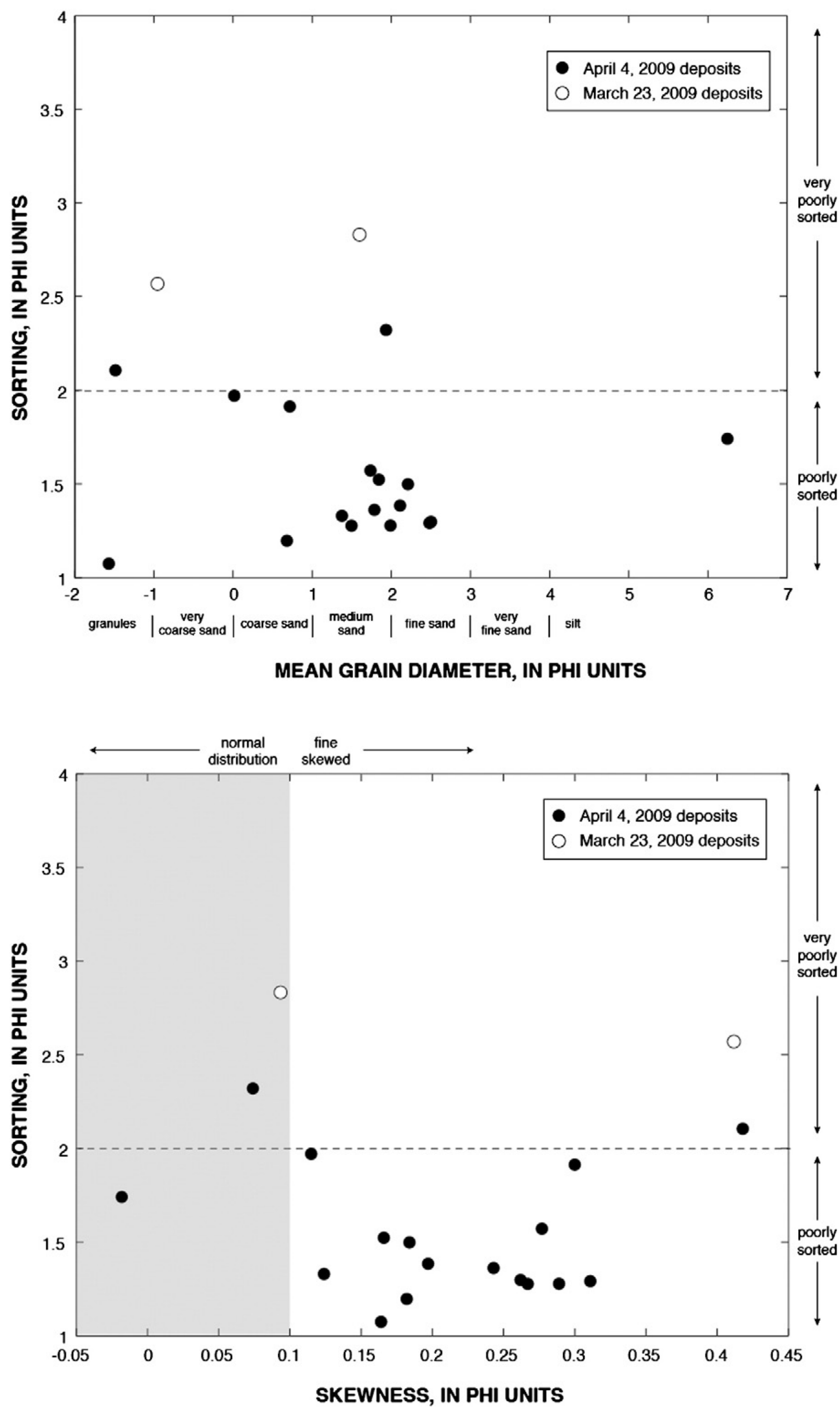

Fig. 16. Plots showing sorting versus mean grain diameter, and sorting versus skewness for matrix samples of lahar deposits emplaced on March 23 and April 4, 2009.

in rivers (Beltaos, 2008). Water stored behind an ice jam can be released suddenly and produce significant flood waves or surges consisting of fragmented, highly concentrated masses of ice and water known as "ice runs" (Jasek, 2003). Ice runs may be unimpeded if they encounter open water downstream, or be impeded if they encounter intact ice cover downstream. A sudden release of water by the eruptive events of March 23 is possibly analogous to the release of an ice jam, and the subsequent formation of the ice-rich lahar analogous to an impeded ice run. Impeded ice runs progress downstream as moving masses of ice rubble, and they can push through and incorporate intact ice or stop and create a new ice jam. The March 23 lahar possibly developed as meltwater and rafted glacier ice encountered the frozen, snow-covered floor of the Drift River valley and formed a temporary ice jam. If such a jam or jams formed and failed, the flow may have behaved as an ice run and formed the ice-rich deposit we observed, which looked similar to the chaotic assemblages of river ice associated with severe ice jam floods (Beltaos, 2008).

Dome-building eruptions that produce pyroclastic flows when the Drift glacier is near or at its full modern volume of about 1 km^3 can

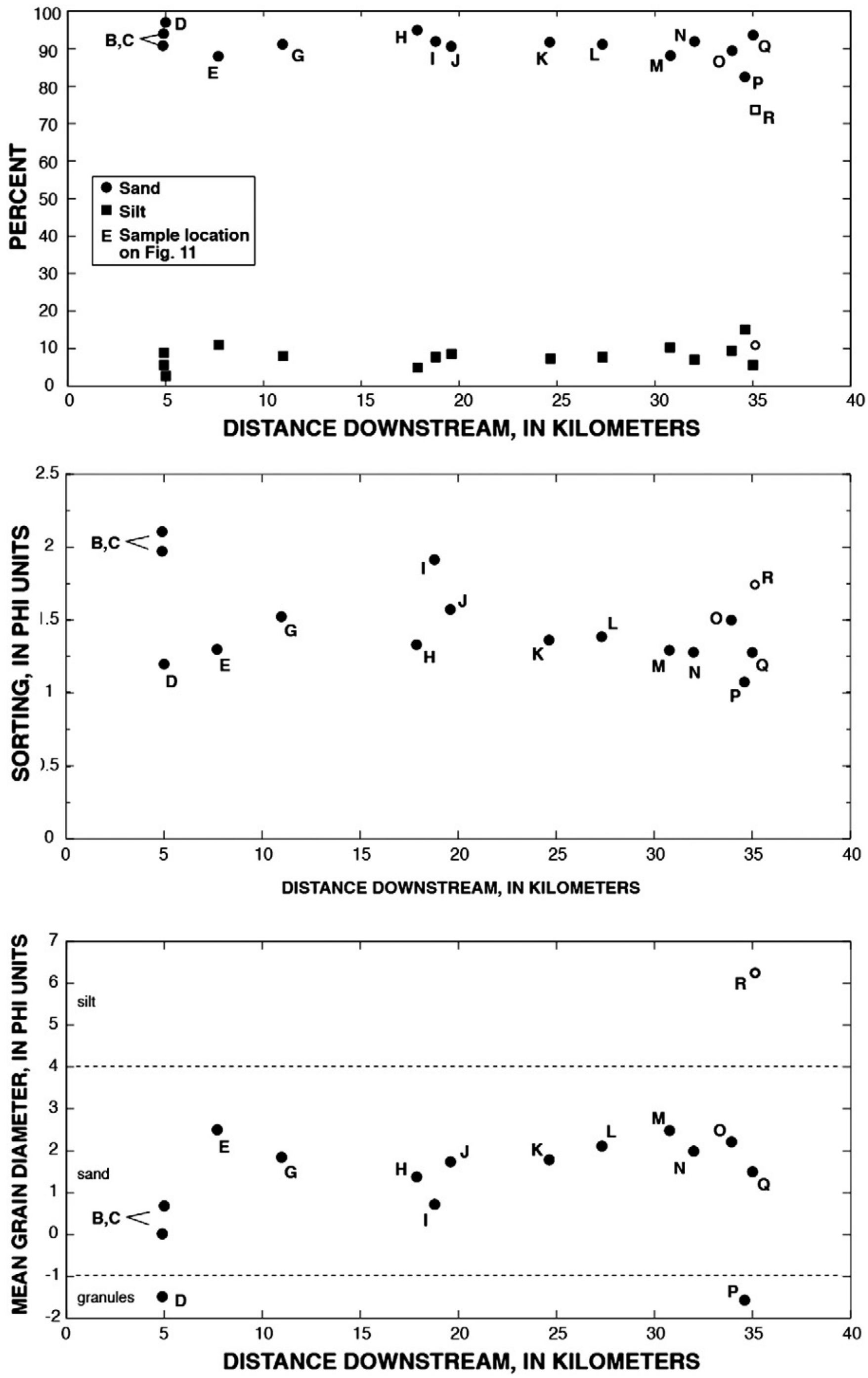

Fig. 17. Percent sand, silt, sorting, and mean grain diameter of April 4, 2009 lahar deposit versus distance downstream. The sample denoted by an open symbol and labeled R was collected from the distal northern margin of the lahar deposit where the flow was tranquil. Letter labels on sample points refer to locations given in Fig. 13, data from sites A and F are March 23 deposits and are not included.

produce sufficient external water to generate large lahars in the Drift River valley. The pyroclastic flows need not be especially large to produce meltwater because glacier ice and snow are readily available in the upper Drift River valley. Throughout the course of historical eruptions, ice has been repeatedly removed from the gorge of the upper Drift glacier above an altitude of about 700 m by pyroclastic flows and dome-collapse debris (Trabant et al., 1994). When ice in the gorge is gone, the only significant source of meltwater for large lahars is the piedmont lobe of the glacier, an area of the valley that has a low surface slope and is not topographically restricted. Pyroclastic flows that reach the piedmont lobe could spread laterally and would be less spatially concentrated unless funneled into ice canyons. Thus, after ice is removed from the gorge area, considerably larger, longer run-out pyroclastic flows may be required to produce meltwater sufficient for large lahars. However, much of the piedmont lobe has a cover of supraglacial debris that could restrict thermal and mechanical erosion by pyroclastic flows. Thus, as eruptions progress, potential water sources may diminish and lessen the ability of an eruption to generate lahars (Trabant et al., 1994).

The volumes and peak discharges of the 2009 lahars were of the same order of magnitude as the 1989–90 lahars, and probably also the 1966 lahars. The largest lahars had volumes of about 10^7–10^8 m^3 and

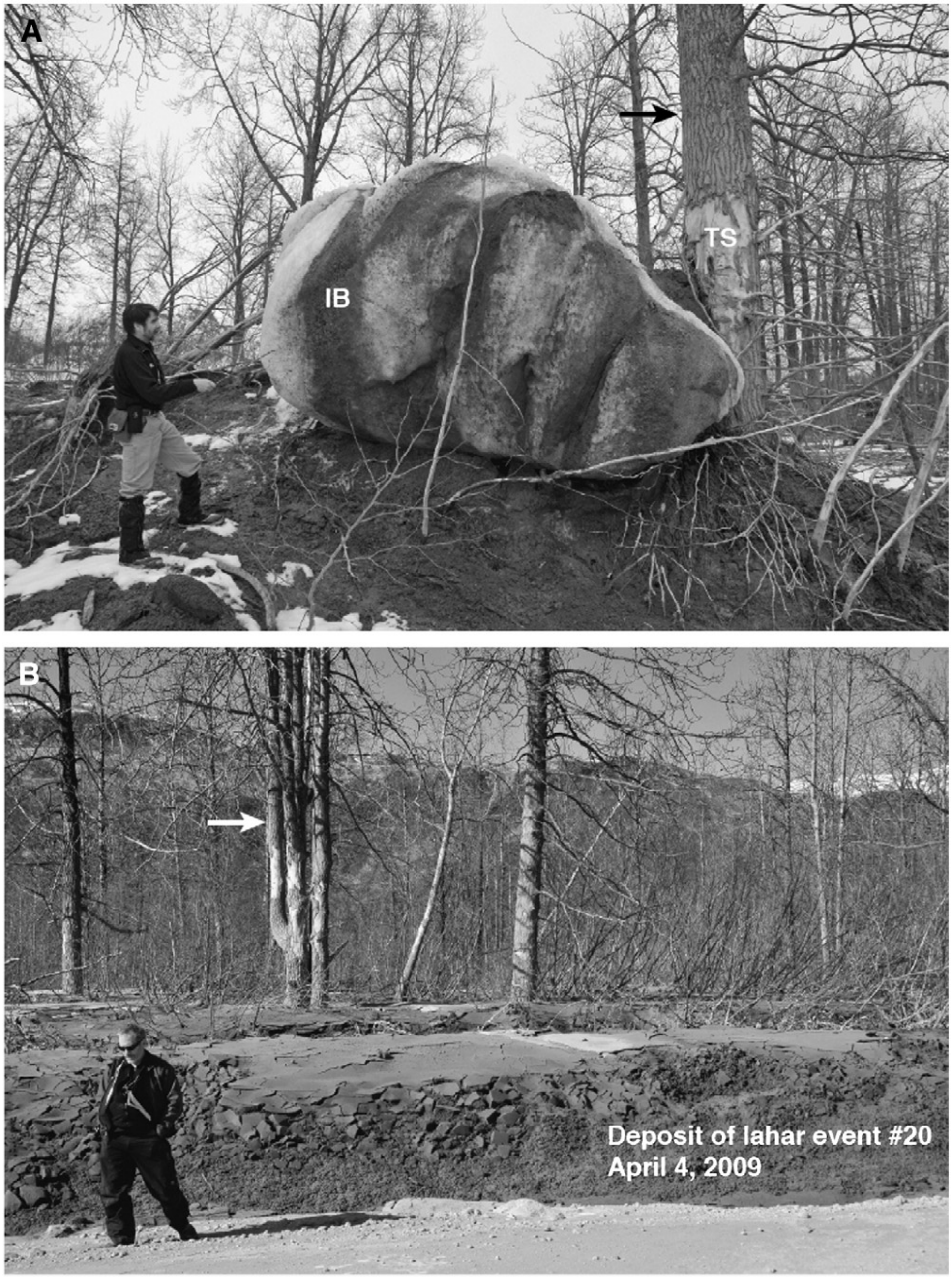

Fig. 18. Examples of high water marks and deposits emplaced by lahar 20, April 4, 2009. Location of photographs is shown in Fig. 13. A) Arrow indicates position of mud line on tree, which records flow run up. Note tree scar (TS) probably caused by ice within the flow. The particle labeled IB is a boulder of glacier ice resting on top of a terminal moraine in the middle Drift River valley about 14 km downstream of the terminus of the Drift glacier. The top of the moraine is about 8 m above the active channel of the Drift River and was over-topped by the lahar. The highest high-water mark of lahar event 20 at this location estimated by the height of mud lines (arrow) above the active channel is 10 m. B) Sandy lahar deposits from lahar event 20 and mud line high water mark on tree (arrow) about 7 m above active channel. This site is located in the middle of the Drift River valley about 17 km downstream of the terminus of the Drift glacier. Photographs by C.F. Waythomas, U.S. Geological Survey, Alaska Volcano Observatory, April 2009.

achieved peak discharges up to 10^4–10^5 $m^3\,s^{-1}$. The total number of smaller lahars triggered also was roughly similar for the two eruptions—at least 18 in 1989–90 (Brantley, 1990) and 20 in 2009.

Significantly larger lahars could be generated by eruptions of a scale much greater than those witnessed historically. Voluminous lahars associated with debris avalanches could be generated by sector collapses of part of the volcanic edifice, and some evidence exists that this has happened possibly several times in the past 10,000 years (Riehle et al., 1981; Beget and Nye, 1994). Lahars larger than those of the past three historical eruptions also might accompany a more voluminous and longer duration explosive eruption. Pyroclastic flows sweeping a broader area of snow and ice in the Drift River basin could generate significantly larger meltwater and lahar volumes (Waythomas et al., 1997).

The degree of hazard in the lower Drift River valley is not simply a function of lahar magnitude, however. A series of smaller lahars and floods could incrementally aggrade the valley floor by transporting and depositing massive volumes of sediment. Such aggradation would clog existing channels and allow subsequent smaller flows to reach higher levels. Furthermore, aggradation can lead to lateral shifting of the river. Lateral shifting could allow flows to more directly impinge on protective structures at the DRMT, or lead to significant channel avulsion as occurred in 1990 when flow from the Drift River entered Montana Bill Creek resulting in scour of channels that

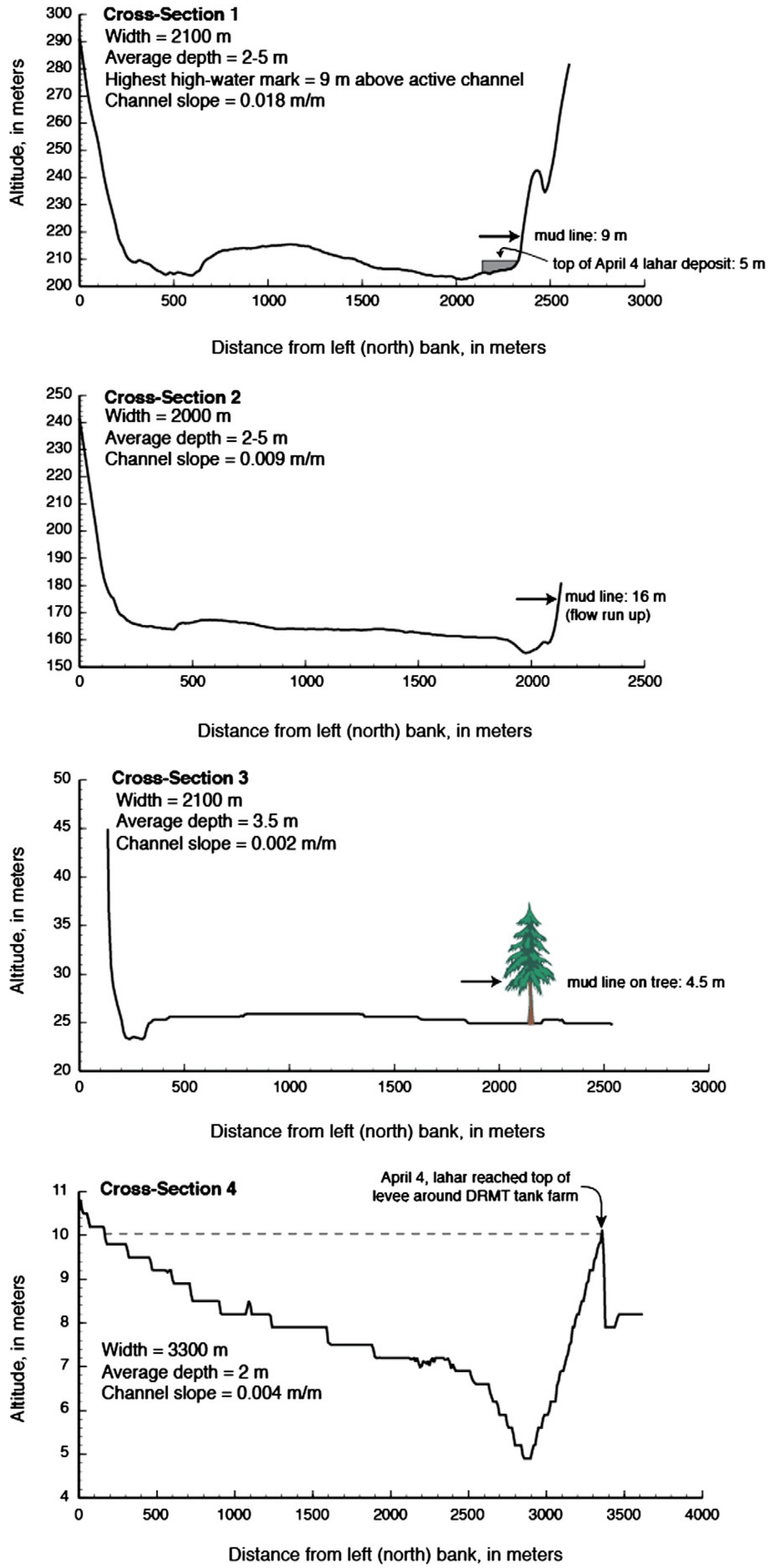
Cross-Section 1
Width = 2100 m
Average depth = 2-5 m
Highest high-water mark = 9 m above active channel
Channel slope = 0.018 m/m
mud line: 9 m
top of April 4 lahar deposit: 5 m
Altitude, in meters
Distance from left (north) bank, in meters
Cross-Section 2
Width = 2000 m
Average depth = 2-5 m
Channel slope = 0.009 m/m
mud line: 16 m
(flow run up)
Distance from left (north) bank, in meters
Cross-Section 3
Width = 2100 m
Average depth = 3.5 m
Channel slope = 0.002 m/m
mud line on tree: 4.5 m
Altitude, in meters
Distance from left (north) bank, in meters
Cross-Section 4
April 4, lahar reached top of
levee around DRMT tank farm
Width = 3300 m
Average depth = 2 m
Channel slope = 0.004 m/m
Altitude, in meters
Distance from left (north) bank, in meters

Table 3
Discharge estimates for lahar 20 of April 4, 2009. Locations of cross sections are shown in Fig. 13. (km, kilometers; m, meters; v, velocity; m/s, meters per second).

Valley reach	Cross section	Distance (km)	Width (m)	Average depth (m)	Channel slope (m/m)	Discharge ($\times 10^3$ m^3 s^{-1})			
						v = 1 m/s	v = 5 m/s	v = 10 m/s	v = 15 m/s
Upper	1	3	2100	2–5	0.018	–	–	42–105	63–157
Upper	2	5	2000	2–5	0.009	–	–	40–100	60–150
Lower	3	26	2100	3.5(?)	0.002	7.4	37	–	–
Lower	4	33	3300	2	0.004	6.6	33	–	–
Lower	4	33	1600	2	0.004	3.2	16	–	–

Table 4
Lahar volume estimates (in bold).

Lahars	(A)	(B)
	Deposit area (km^2) × average deposit thickness (m) = volume (m^3)	Ice-loss volume × 0.9 × bulking factor = volume (m^3)
Lahars 2 and 3 March 23	100 × 0.2–2 = **2 × 10^7^–2 × 10^8^**	0.5–1.5 × 10^8 m^3 of ice, a portion of which was water that mobilized flow of mostly ice volume = **0.5–1.5 × 10^8 m^3**
Lahars 5 and 6 March 26	65 × 0.2–1 = **1–6 × 10^7**	
Lahar 20 April 4	125 × 0.5–2 = **6 × 10^7–2.5 × 10^8**	0.5–1 × 10^8 m^3 ice = 0.5–0.9 × 10^8 m^3 water × 1.5–2 = **7.5 × 10^7–2 × 10^8**

crossed the buried pipeline that delivers oil to the DRMT (Dorava and Meyer, 1994).

Huge quantities of sediment were mobilized by lahars in the Drift River valley during the 2009 eruption. By the summer of 2010, as much as 10 m of incision through the 2009 lahar deposits (and possibly the underlying alluvium) had occurred in the upper Drift River valley. This channel incision contributed additional sediment downstream, the overall result of which was several meters of aggradation of the lower Drift River and the Rust Slough–Cannery Creek drainage. As the Drift River erodes and redistributes the material deposited by the lahars, downstream aggradation, and possibly river avulsion, is likely to continue for many years, which may induce higher than usual river stages and flooding along the lower Drift River and its distributary channels.

Eruption-induced lahars in the Drift River valley are much larger than the flows that can be produced by rainfall runoff. Documented flood peaks in drainages throughout south-central Alaska (Jones and Fahl, 1994) provide a general estimate for the largest meteorologically generated flows possible in the region (Fig. 20), and indicate a maximum water-flood peak discharge of about 2000 m^3 s^{-1} for the Drift River (drainage area = 570 km^2). Using regional flood-frequency equations described in Curran et al. (2003), the estimated 100-year and 500-year-flood peak discharges for the Drift River drainage are about 1000 m^3 s^{-1} and 1300 m^3 s^{-1}, which are tens to hundreds of times smaller than historical Redoubt lahars. The estimated peak discharge of the April 4 lahar near the DRMT (Fig. 13, cross-section 4), which is more directly comparable to the regional flood-frequency estimate of the 100 year flood peak, was 3000–33,000 m^3 s^{-1} and at least 3–30 times larger than the estimated 100-year flood peak. Clearly, eruption-generated flow discharges can be much larger than those generated by rainfall or normal snowmelt.

7. Conclusions

Redoubt Volcano has produced large (discharges to 10^4 m^3 s^{-1} and volumes to 10^7 m^3) to very large (discharges to 10^5 m^3 s^{-1} and volumes to 10^9 m^3) lahars of varying character during recent eruptions in 2009, 1989–90 and 1966–68. These lahars were triggered by the rapid melting of snow and ice on Drift glacier by explosive events and pyroclastic flows resulting from collapses of growing lava domes and possibly from eruption column collapse. This volcano is capable of producing voluminous lahars in part because the topography of its upper northern flank concentrates pyroclastic flows into a narrow, steep bedrock gorge that is occupied by the upper part of Drift glacier. This allows large volumes of snow and ice to be entrained and melted rapidly. Glacier ice removed during eruptions generally regenerates in about 10 years.

The primary conclusions of our analysis of lahar generation during the 2009 eruption are:

1) Explosive activity from March 23 to April 4 produced lahars having volumes of 10^7–10^8 m^3 and peak discharges of 10^4–10^5 m^3 s^{-1}—flows almost two orders of magnitude larger than can be generated by rainstorms or seasonal snowmelt in this region and comparable in size to the largest lahars generated during previous historical eruptions. Even larger lahars could be generated by structural failure of the volcanic edifice (sector collapse), or by pyroclastic flows larger than those documented during the 1989–90 and 2009 eruptions.
2) Two very large lahars, generated only hours apart at the beginning of the explosive phase of the eruption on March 23, were water-saturated granular mass flows composed primarily of ice fragments and water (ice-slurry lahars). These two lahars covered most of the Drift River valley floor and flowed about 35 km from Drift glacier to Cook Inlet. Volcanically generated ice-slurry lahars of this magnitude are unusual and apparently unprecedented in the literature.
3) The very large lahar generated on April 4 at the end of the explosive phase of the eruption contained relatively little ice; it was a more dilute hyperconcentrated-flow lahar. Deposits of this lahar mostly consist of medium to fine sand with abundant fragments of juvenile andesite
4) In addition to these large to very large lahars, at least 17 additional smaller lahars and floods were generated in late March.

Redoubt Volcano has erupted more than 50 times in the past 10,000 years and 4 times since 1900. Each of three eruptions since the 1960's has produced numerous lahars in the Drift River valley. Another eruption and hazardous lahars down the Drift River during next 20–30 years would not be unusual or unexpected.

Fig. 19. Representative pre-eruption cross sections of the upper (cross-sections 1 and 2) and lower (cross-sections 3 and 4) Drift River valley. Data used to generate cross sections were obtained from a DEM made from August 1990 topographic maps of the Drift River valley. Flow depth at cross-section 4, indicated by dashed horizontal line, is based on measurements of the height of mud lines on trees above the nearest active channel.

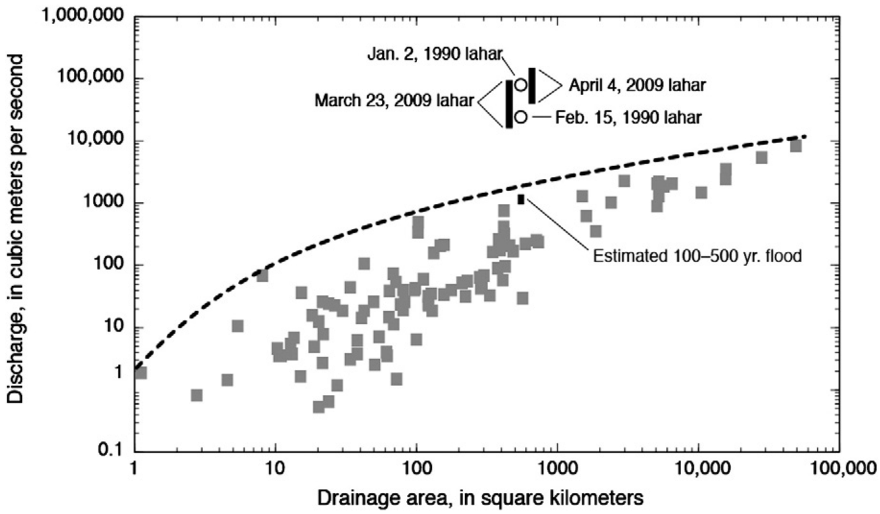

Fig. 20. Peak discharge versus drainage area for meteorologically generated floods in south-central Alaska (from Jones and Fahl, 1994), compared to peak discharge of the largest lahars of the 1989–90 and 2009 eruptions of Redoubt volcano. The estimated peak discharge of the 100- and 500-year floods in the Drift River basin as determined using regional flood-frequency equations in Curran et al. (2003) also is shown. The dashed line is an envelope curve indicating the largest known peak flows relative to drainage basin area.

In addition to their direct impacts, lahars can have secondary impacts on valley morphology and fluvial processes. Incision of lahar deposits in the upper and middle parts of the Drift River valley has supplied sediment leading to distal channel aggradation, and bed elevations in the lower Drift River valley have risen by several meters. Continued aggradation of the lower Drift River will maintain elevated channel beds and promote overbank flooding during periods of high runoff, or should eruptive activity resume, during even small- to moderate-sized lahars.

Acknowledgments

The authors thank the staff of Lake Clark National Park and Preserve for facilitation of our work within the park. We appreciate and gratefully acknowledge the support of the staff and operators of the Drift River Marine Terminal. Manuscript reviews provided by Dave Meyer and Game McGimsey and discussions with Kate Bull, Kristi Wallace, Chris Nye, and Bob Swenson helped clarify several aspects of the work.

References

Beget, J.E., Nye, C.J., 1994. Postglacial eruption history of Redoubt Volcano, Alaska. Journal of Volcanology and Geothermal Research 62, 31–54.

Beltaos, S., 2008. River Ice Breakup. Water Resources Publications, Highlands Ranch, CO. 480 pp.

Bleick, H.A., Coombs, M.L., Cervelli, P.F, Bull, K.F., Wessels, R.L., 2013. Volcano–ice interactions precursory to the 2009 eruption of Redoubt Volcano, Alaska. Journal of Volcanology and Geothermal Research 259, 373–388.

Brantley, S.R. (Ed.), 1990. The eruption of Redoubt Volcano, Alaska, December 14, 1989–August 31, 1990U.S. Geological Survey Circular 1061 33 pp.

Bull, K.F., Buurman, H., 2013. An overview of the 2009 eruption of Redoubt Volcano, Alaska. Journal of Volcanology and Geothermal Research 259, 2–15.

Buurman, H., West, M., Thompson, G., 2013. The seismicity of the 2009 Redoubt eruption. Journal of Volcanology and Geothermal Research 259, 16–30.

Coombs, M.L., Sisson, T.W., Bleick, H., Henton, S., Nye, C.J., Payne, A., Cameron, C., Larsen, J.F., Wallace, K.L., Bull, K.F., 2013. Andesites of the 2009 eruption of Redoubt Volcano, Alaska. Journal of Volcanology and Geothermal Research 106, 349–372.

Cronin, S.J., Neall, V.E., Lecointre, J.A., Palmer, A.S., 1996. Unusual “snow slurry” lahars from Ruapehu volcano, New Zealand, September 1995. Geology 24, 1107–1110.

Curran, J.H., Meyer, D.F., Tasker, G.D., 2003. Estimating the magnitude and frequency of peak streamflows for ungaged sites on streams in Alaska and conterminous basins in Canada. U.S. Geological Survey Water-Resources Investigations Report 03-4188. 101 pp.

Diefenbach, A.K., Bull, K.F., Wessels, R.L., McGimsey, R., 2013. Photogrammetric monitoring of lava dome growth during the 2009 eruption of Redoubt Volcano. Journal of Volcanology and Geothermal Research 259, 308–316.

Dorava, J.M., Meyer, D.F., 1994. Hydrologic hazards in the lower Drift River basin associated with the 1989–90 eruptions of Redoubt Volcano, Alaska. Journal of Volcanology and Geothermal Research 62, 387–407.

Gardner, C.A., Neal, C.A., Waitt, R.B., Janda, R.J., 1994. Proximal pyroclastic deposits from the 1989–1990 eruption of Redoubt volcano, Alaska—stratigraphy, distribution, and physical characteristics. Journal of Volcanology and Geothermal Research 62, 213–250.

Iverson, R.M., LaHusen, R.G., Major, J.J., Zimmerman, C.L., 1994. Debris flow against obstacles and bends: dynamics and deposits. Eos 75, 274.

Jakob, M., 2005. A size classification for debris flows. Engineering Geology 79, 151–161.

Jasek, M., 2003. Ice jam release surges, ice runs, and breaking fronts: field measurements, physical descriptions, and research needs. Canadian Journal of Civil Engineering 30, 113–127.

Jones, S.H., Fahl, C.B., 1994. Magnitude and frequency of floods in Alaska and conterminous basins of Canada. U.S. Geological Survey Water-Resources Investigations Report 93-4179. 122 pp.

Kilgour, G., Manville, V., Della Pasqua, F., Graettinger, A., Hodgson, K.A., Jolly, G.E., 2010. The 25 September 2007 eruption of Mount Ruapehu, New Zealand: directed ballistics, surtseyan jets, and ice-slurry lahars. Journal of Volcanology and Geothermal Research 191, 1–14.

Lube, G., Cronin, S.J., Procter, J.N., 2009. Explaining the extreme mobility of volcanic ice-slurry flows, Ruapehu volcano, New Zealand. Geology 37, 15–18.

Major, J.J., Newhall, C.G., 1989. Snow and ice perturbation during historical volcanic eruptions and the formation of lahars and floods. Bulletin of Volcanology 52, 1–27.

Major, J.J., Pierson, T.C., Scott, K.M., 2005. Debris flows at Mount St. Helens, Washington, USA. In: Jakob, M., Hungr, O. (Eds.), Debris-flow Hazards and Related Phenomena. Springer-Praxis, Chichester, UK, pp. 685–731.

Miller, T.P., 1994. Dome growth and destruction during the 1989–1990 eruption of Redoubt volcano. Journal of Volcanology and Geophysical Research 62, 197–212.

Mizuyama, T., Kobashi, S., Ou, G., 1992. Prediction of debris flow peak discharge. Proceedings, International Symposium Interpraevent 4, 99–108.

Mothes, P.A., Hall, M.L., Janda, R.J., 1998. The enormous Chillos Valley lahar: an ash-flow-generated debris flow from Cotopaxi Volcano, Ecuador. Bulletin of Volcanology 59, 233–244.

Pierson, T.C., 1998. An empirical method for estimating the travel times for wet volcanic mass flows. Bulletin of Volcanology 60, 98–109.

Pierson, T.C., 2005. Hyperconcentrated flow—transitional process between water flow and debris flow. In: Jakob, M., Hungr, O. (Eds.), Debris-flow Hazards and Related Phenomena. Springer, Berlin, pp. 159–202.

Pierson, T.C., Janda, R.J., 1994. Volcanic mixed avalanches: a distinct eruption-triggered mass-flow process at snow-clad volcanoes. Geological Society of America Bulletin 106, 1351–1358.

Pierson, T.C., Janda, R.J., Thouret, J.-C., Borrero, C.A., 1990. Perturbation and melting of snow and ice by the 13 November 1985 eruption of Nevado del Ruiz, Columbia, and consequent mobilization, flow and deposition of lahars. Journal of Volcanology and Geothermal Research 41, 17–66.

Rickenmann, D., 1999. Empirical relationships for debris flows. Natural Hazards 19, 47–77.

Riehle, J.R., Kienle, J., Emmel, K.S., 1981. Lahars in Crescent River Valley, Lower Cook Inlet, Alaska. Alaska Division of Geological and Geophysical Surveys Geologic Report 53 (10 pp.).

Schaefer, J.R. (Ed.), 2012. The 2009 eruption of Redoubt Volcano, AlaskaAlaska Division of Geological and Geophysical Surveys Report of Investigation 2011–2015.

Schiff, C.J., Kaufman, D.S., Wallace, K.L., Ketterer, M.E., 2010. An improved tephrochronology of Redoubt Volcano, Alaska. Journal of Volcanology and Geothermal Research 193, 203–214.

Scott, K.M., 1988. Origins, behavior, and sedimentology of lahars and lahar-runout flows in the Toutle–Cowlitz River system. U.S. Geological Survey Professional Paper 1447-A.

Scott, K.M., Janda, R.J., de la Cruz, E., Gabinete, E., Eto, I., Isada, M., Sexton, M., Hadley, K.C., 1996. Channel and sedimentation responses to large volumes of 1991 volcanic deposits on the east flank of Mount Pinatubo. In: Newhall, C.G., Punongbayan, R.S. (Eds.), Fire and Mud, Eruptions and Lahars of Mount Pinatubo, Philippines. University of Washington Press, pp. 971–988.
Sturm, M., Benson, C., MacKeith, P., 1986. Effects of the 1966–68 eruptions of Mount Redoubt on the flow of Drift Glacier, Alaska, U.S.A. Journal of Glaciology 32, 355–361.
Till, A.B., Yount, M.E., Bevier, M.L., 1994. The geologic history of Redoubt Volcano, Alaska. Journal of Volcanology and Geothermal Research 62, 11–30.
Trabant, D., Hawkins, D.B., 1997. Glacier ice-volume modeling and glacier volumes on Redoubt Volcano, Alaska. U.S. Geological Survey Water-Resources Investigations Report 97-4187. 29 pp.
Trabant, D.C., Waitt, R.B., Major, J.J., 1994. Disruption of Drift glacier and origin of floods during the 1989–1990 eruptions of Redoubt Volcano, Alaska. Journal of Volcanology and Geothermal Research 62, 369–385.
Vallance, J.W., 2000. Lahars. In: Sigurdsson, H., Houghton, B.F., McNutt, S.R., Rymer, H., Stix, J. (Eds.), Encyclopedia of Volcanoes. Academic Press, pp. 601–616.
Waitt, R.B., Pierson, T.C., MacLeod, N.S., Janda, R.J., Voight, B., Holcomb, R.T., 1983. Eruption-triggered avalanche, flood, and lahar at Mount St. Helens—effects of winter snowpack. Science 221, 1394–1396.
Waitt, R.B., Gardner, C.A., Pierson, T.C., Major, J.J., Neal, C.A., 1994. Unusual ice diamicts emplaced during the December 15, 1989, eruption of Redoubt Volcano, Alaska. Journal of Volcanology and Geothermal Research 62, 409–428.
Walder, J.S., 2000a. Pyroclast/snow interactions and thermally driven slurry formation. Part 1: theory for monodisperse grain beds. Bulletin of Volcanology 62, 105–118.
Walder, J.S., 2000b. Pyroclast/snow interactions and thermally driven slurry formation. Part 2: experiments and theoretical extension to polydisperse tephra. Bulletin of Volcanology 62, 119–129.
Wallace, K.L., Schaefer, J.R., Coombs, M.L., 2013. Character,mass, distribution, and origin of tephra-fall deposits from the 2009 eruption of Redoubt Volcano, Alaska—Highlighting the significance of particle aggregation. Journal of Volcanology and Geothermal Research 259, 145–169.
Waythomas, C.F., Dorava, J.M., Miller, T.P., Neal, C.A., McGimsey, R.G., 1997. Preliminary volcano-hazard assessment for Redoubt Volcano, Alaska. U.S. Geological Survey Open-File Report OF 97-857. 40 pp.